Computers and Mathematics with Applications 152 (2023) 341–354

Contents lists available at ScienceDirect

Computers and Mathematics with Applications

journal homepage: www.elsevier.com/locate/camwa

A cVEM-DG space-time method for the dissipative wave equation

Paola F. Antonietti, Francesca Bonizzoni *, Marco Verani

MOX, Department of Mathematics, Politecnico di Milano, Piazza Leonardo da Vinci 32, Milano, 20133, Italy

ARTICLE INFO

Keywords:
Damped wave equation
Space-time discretization
Tensor product discretization
Virtual element method
Discontinuous Galerkin method
Stability and convergence analysis

ABSTRACT

A novel space-time discretization for the (linear) scalar-valued dissipative wave equation is presented. It is a structured approach, namely, the discretization space is obtained tensorizing the Virtual Element (VE) discretization in space with the Discontinuous Galerkin (DG) method in time. As such, it combines the advantages of both the VE and the DG methods. The proposed scheme is implicit and it is proved to be unconditionally stable and accurate in space and time.

1. Introduction

In this paper we propose a space-time Virtual Element/Discontinuous Galerkin method for the (linear) scalar-valued dissipative wave equation in two- and three-dimensions. The method is based on Virtual Element (VE) for space discretization coupled with discontinuous Galerkin (DG) finite element method for the time integration of the resulting second-order ordinary differential system. The model problem considered in this paper serves as a prototype model for the vector-valued (damped) elastic wave equation typically encountered in geophysical applications.

The Virtual Element method (VEM) has been introduced in [1] for elliptic problems. VEMs for linear and nonlinear elasticity have been developed in [2–4], whereas VEMs for parabolic, plate bending, Cahn-Hilliard, Stokes, Helmholtz and Laplace-Beltrami problems have been addressed in [5–10]. VEMs for the space discretization of wave-type problems have been addressed in [11–14].

Concerning time-integration of second-order differential systems stemming from space discretization of wave-type problems, classically, time marching schemes are based on (either implicit or explicit) finite differences approaches, e.g., we refer to [15,16] for a general overview. On the other hand, space-time finite element methods for second-order hyperbolic equations have been largely developed, thanks to their ability to achieve high-order approximations in both space and time, to accurately capture steep fronts, and their firm mathematical foundation, where stability and convergence can be proved.

Among space-time finite element methods, we can distinguish between "structured" and "unstructured" numerical approaches. In "structured" approaches, the space-time grid is obtained as tensor product of space and time meshes; a non-exhaustive list of approaches includes [17–21]. For such formulations, $h-$, $p-$ or $hp-$ adaptive refinement of the space-time domain can be developed and implemented, see, e.g., [22,23]. On the other hand, "unstructured" techniques, see, e.g., the seminal works [24,25] make use of full space-time meshes, where time is treated as an additional dimension, see [26–28] for examples, and the recent contribution [29]. Among unstructured methods, we also mention Trefftz-type techniques [30–34], in which the numerical solution is looked for in the Trefftz space, and the tent-pitching paradigm [35], in which the space-time elements are progressively built on top of each other in order to grant stability of the numerical scheme. Recently, in [33,34] a combination of Trefftz and tent-pitching techniques has been proposed with application to first order hyperbolic problems. A tent-pitching scheme motivated by Friedrichs' theory can be found in [36].

The DG approach has been extensively used to approximate initial-value problems, where the DG paradigm shows certain advantages with respect to other implicit schemes such as the Johnson's method, see e.g. [37,38]. Indeed, thanks to the DG paradigm, the solution at time-slab $[t_n, t_{n+1}]$ depends only on the solution at the time instant t_n^-. The use of DG methods in both space and time dimensions leads to a fully DG space-time formulation such as e.g., [39–41,21].

Finally, a typical approach for second order differential equations consists in reformulating them as a system of first order hyperbolic equations. Thus, velocity is considered as an additional problem's unknown, yielding to doubling the dimension of the final linear system, cf. [39,24,42,37,43,44].

* Corresponding author.
E-mail addresses: paola.antonietti@polimi.it (P.F. Antonietti), francesca.bonizzoni@polimi.it (F. Bonizzoni), marco.verani@polimi.it (M. Verani).

https://doi.org/10.1016/j.camwa.2023.10.022
Received 30 March 2023; Received in revised form 10 October 2023; Accepted 15 October 2023

In this work we present a novel structured VEM/DG formulation that combines the VE advantages for space discretization together with those of the DG methods for time integration. The obtained scheme is implicit, unconditionally stable and provides an accurate approximation with respect to both space and time discretization errors. Throughout the paper we will use the notation $x \lesssim y$ with the meaning $x \le cy$, with c positive constant independent of the discretization parameters.

The paper is organized as follows. In Section 2 we introduce the problem; its semi-discrete VEM approximation is discussed in Section 3, and in Section 4 we present DG discretization in time. Section 5 introduces the fully-discrete VEM-DG formulation and studies its well-posedness and stability, whereas in Section 6 we prove *a priori* error estimates in a suitable energy norm. Finally, in Section 7, the method is validated through several numerical experiments in two dimensions (in space).

2. Problem setting

Let $\Omega \subset \mathbb{R}^d$, $d = 2, 3$, be an open bounded convex polygonal domain. The problem we are interested reads as follows: for $T > 0$, find $u : \Omega \times (0, T] \to \mathbb{R}$ such that

$$\begin{cases} u_{tt} + \nu u_t - \Delta u = f, & \text{in } \Omega \times (0,T], \\ u = 0, & \text{on } \partial\Omega \times (0,T], \\ u(\cdot,0) = u_0,\ u_t(\cdot,0) = z_0, & \text{in } \Omega, \end{cases} \tag{2.1}$$

where $\nu \in \mathbb{R}^+$ is the dissipation coefficient, f is the external force, u_0 and z_0 are the initial data, and u_t, u_{tt} denote the first and second order time derivative of the unknown function u, respectively. Note that, by little modifications, our analysis extends to the case of (positive) bounded dissipation function $\nu \in L^\infty(\Omega)$. By standard arguments, we derive the variational formulation of (2.1): given $f \in L^2(\Omega \times (0,T))$ and $u_0, z_0 \in H^1_0(\Omega)$, find $u \in C^0\left(0,T; H^1_0(\Omega)\right) \cap C^1\left(0,T; L^2(\Omega)\right)$ such that, for all $v \in H^1_0(\Omega)$ and for a.e. $t \in (0,T)$

$$\left(u_{tt}(t), v\right)_{L^2(\Omega)} + \nu \left(u_t(t), v\right)_{L^2(\Omega)} + a(u(t), v) = \left(f(t), v\right)_{L^2(\Omega)}, \tag{2.2}$$

supplemented with the initial conditions $u(\cdot,0) = u_0$, $u_t(\cdot,0) = z_0$, where $(\bullet,\bullet)_{L^2(\Omega)}$ denotes the $L^2(\Omega)$-inner product, and $a : H^1_0(\Omega) \times H^1_0(\Omega) \to \mathbb{R}$ is defined as $a(w,v) = (\nabla w, \nabla v)_{L^2(\Omega)}$. Following [45] it is possible to prove existence and uniqueness of the solution to problem (2.2).

Remark 2.1. Note that we assume Ω to be convex in order to prove optimal L^2-error estimates. However, the proposed method can be applied without modifications to non-convex domains, yielding suboptional theoretical convergence rates in the L^2-norm.

3. Space discretization based on the VEM

In this section we apply the VEM to discretize problem (2.2) in space. In particular, we follow [11], where the VE space discretization of (2.2) with damping $\nu = 0$ is introduced. We start recalling the ingredients of the VEM that we will need, with focus on the two-dimensional case (the three-dimensional case being analogous but more technical). For a complete presentation, we refer to [1,46,47].

3.1. VE space

Let $\mathcal{T}_h$ be a (not necessarily conforming) decomposition of Ω into n_P non-overlapping (open) polygons E_ℓ with flat faces, i.e., $\bar\Omega = \cup_{\ell=1}^{n_P} \bar E_\ell$ with $E_\ell \cap E_{\ell'} = \emptyset$ for $\ell \neq \ell'$. Let $h_E := \mathrm{diam}(E)$ and $h := \max_{E \in \mathcal{T}_h} h_E$. In the following, we assume that (i) each element $E \in \mathcal{T}_h$ is star-shaped with respect to a ball of radius γh_E; (ii) the distance between any two vertices of E is larger than $c h_E$, for $\gamma, c > 0$ constants independent of h and E.

Let $k \in \mathbb{N}$ denote the polynomial degree of the method. For any fixed $E \in \mathcal{T}_h$, we introduce the following notations:

(i) $\mathbb{P}_k(E)$ is the set of polynomials on E of total degree less or equal to k;

(ii) $\mathbb{B}(\partial E) := \{v \in C^0(\partial E) \text{ s.t. } v|_e \in \mathbb{P}_k(e) \text{ for all edge } e \subset \partial E\}$;

(iii) $\Pi^{\nabla,E} : H^1(E) \to \mathbb{P}_k(E)$ is the energy projection operator defined by

$$a^E(q_k, w - \Pi^{\nabla,E} w) = 0 \quad \forall q_k \in \mathbb{P}_k(E), \tag{3.1}$$

where $a^E : H^1(E) \times H^1(E) \to \mathbb{R}$ is the local counterpart of the bilinear form $a(\bullet,\bullet)$, namely, $a^E(v,w) = \int_E \nabla v \cdot \nabla w \, \mathrm{d}x$ for all $v, w \in H^1(E)$, and $a(v,w) = \sum_{E \in \mathcal{T}_h} a^E(v,w)$ for all $v, w \in H^1(\Omega)$. To fix the constant in the definition (3.1) of $\Pi^{\nabla,E} w$, we further require

$$\begin{cases} \dfrac{1}{|\partial E|} \displaystyle\int_{\partial E} (w - \Pi^{\nabla,E} w) \, \mathrm{d}s = 0, & \text{for } k = 1, \\ \dfrac{1}{|E|} \displaystyle\int_E (w - \Pi^{\nabla,E} w) \, \mathrm{d}x = 0, & \text{for } k > 1; \end{cases}$$

(iv) $\Pi^{0,E} : L^2(E) \to \mathbb{P}_k(E)$ is the L^2-orthogonal projection operator defined by

$$\left(q_k, w - \Pi^{0,E} w\right)_{L^2(E)} = 0 \quad \forall q_k \in \mathbb{P}_k(E). \tag{3.2}$$

There exists a positive constant C such that, for all $u \in H^{s+1}(E)$ with $0 \le s \le k$, there holds

$$\left\| u - \Pi^{0,E} u \right\|_{L^2(E)} \le C h_E^{s+1} |u|_{H^{s+1}(E)}, \tag{3.3}$$

where h_E is the diameter of the element E. (See [48].)

We can now introduce the (local) enhanced VE space

$$W_h^E := \left\{ w \in V_h^E \text{ s.t. } \left(w - \Pi^{\nabla,E} w, q\right)_{L^2(E)} = 0 \text{ for all } q \in \mathbb{P}_k(E)/\mathbb{P}_{k-2}(E) \right\}, \tag{3.4}$$

where V_h^E denotes the (local) augmented VE space

$$V_h^E := \left\{ w \in H^1(E) \text{ s.t. } w \in \mathbb{B}_k(\partial E) \text{ and } \Delta w \in \mathbb{P}_k(E) \right\},$$

and $\mathbb{P}_k(E)/\mathbb{P}_{k-2}(E)$ denotes the set of polynomials of total degree k on E that are L^2-orthogonal to all polynomials of total degree $k-2$ on E (with the convention $\mathbb{P}_{-1} := \emptyset$). Note, in particular, that $\mathbb{P}_k(E) \subset W_h^E(E)$. The space W_h^E is equipped with the following set of (local) degrees of freedom (DOFs):

- nodal values at all n_E vertices of the polygon E;
- nodal values at $k-1$ internal Gauss-Lobatto quadrature points of every edge $e \in \partial E$;
- (for $k \ge 2$) moments up to order $k-2$ in E, namely, for $w \in W_h^E$,

$$\left(w, q_{k-2}\right)_{L^2(E)} \quad \text{for all } q_{k-2} \in \mathbb{P}_{k-2}.$$

In particular, $\dim(W_h^E) = n_E k + \frac{k(k-1)}{2}$. It is important to notice that both the energy projection and the L^2-orthogonal projection operators are computable only on the basis of degrees of freedom above.

The global enhanced VE space is given by

$$W_h := \left\{ v \in H^1_0(\Omega) \text{ s.t. } v|_E \in W_h^E \text{ for all } E \in \mathcal{T}_h \right\}. \tag{3.5}$$

It is equipped with the following set of (global) DOFs:

- nodal values at all n_V vertices of $\mathcal{T}_h$;
- nodal values at $k-1$ internal Gauss-Lobatto quadrature points of all n_e edges of $\mathcal{T}_h$;
- (for $k \ge 2$) moments up to order $k-2$ in all n_P polygons of $\mathcal{T}_h$, namely, for $w \in W_h$,

$$\left(w, q_{k-2}\right)_{L^2(E)} \quad \text{for all } q_{k-2} \in \mathbb{P}_{k-2}(E);$$

and it has dimension $\dim(W_h) = n_V + (k-1)n_e + n_P\frac{k(k-1)}{2}$. In the following, we set $N_h := \dim(W_h)$.

Given a smooth enough function u, we define its VE interpolant u_I as the function in W_h verifying, for all $j = 1, \dots, N_h$

$$\mathrm{dof}_j(u) = \mathrm{dof}_j(u_I), \tag{3.6}$$

where dof_j is the operator associating its argument to the j-th (global) DOF. It can be shown (see, e.g., [52,54,55,53]) that there exists a positive constant C such that, for all $E \in \mathcal{T}_h$, there holds

$$\|u - u_I\|_{L^2(E)} + h\,|u - u_I|_{H^1(E)} \le Ch^{k+1}\,|u|_{H^{k+1}(E)}. \tag{3.7}$$

3.2. VE bilinear forms

Based on the classical observation that, given an arbitrary pair of VE functions $v_h, w_h \in W_h^E$, the quantities $a^E(v_h, w_h)$, $(v_h, w_h)_{L^2(E)}$ can not be computed, we introduce computable approximations $a_h^E, m_h^E : W_h^E \times W_h^E \to \mathbb{R}$, given by

$$\begin{aligned} a_h^E(v_h, w_h) &:= a^E(\Pi^{\nabla,E}v_h, \Pi^{\nabla,E}w_h) + S^E\left((Id - \Pi^{\nabla,E})v_h, (Id - \Pi^{\nabla,E})w_h\right), \\ m_h^E(v_h, w_h) &:= \left(\Pi^{0,E}v_h, \Pi^{0,E}w_h\right)_{L^2(E)} \\ &\quad + R^E\left((Id - \Pi^{0,E})v_h, (Id - \Pi^{0,E})w_h\right), \end{aligned} \tag{3.8}$$

where S^E, $R^E : W_h^E \times W_h^E \to \mathbb{R}$ are symmetric stabilizing bilinear forms fulfilling, for all $v_h\, w_h \in W_h^E$ with $\Pi^{\nabla,E}v_h = 0$, $\Pi^{0,E}w_h = 0$,

$$\begin{aligned} a^E(w_h, w_h) &\lesssim R^E(w_h, w_h) \lesssim a^E(w_h, w_h), \\ (w_h, w_h)_{L^2(E)} &\lesssim S^E(w_h, w_h) \lesssim (w_h, w_h)_{L^2(E)}. \end{aligned} \tag{3.9}$$

In particular, the local virtual bilinear forms defined in (3.8) fulfill the k-consistency and stability properties, namely, for all $q_h \in \mathbb{P}_k(E)$ and $w_h \in W_h^E$

$$a_h^E(q_h, w_h) = a^E(q_h, w_h), \quad m_h^E(q_h, w_h) = m^E(q_h, w_h), \tag{3.10}$$

and

$$\begin{aligned} a^E(w_h, w_h) &\lesssim a_h^E(w_h, w_h) \lesssim a^E(w_h, w_h), \\ (w_h, w_h)_{L^2(E)} &\lesssim m_h^E(w_h, w_h) \lesssim (w_h, w_h)_{L^2(E)}. \end{aligned} \tag{3.11}$$

Remark 3.1. In the numerical experiments, we will approximate the stabilizing forms $S^E(\bullet,\bullet)$, $R^E(\bullet,\bullet)$ with the computable bilinear forms $S_h^E(\bullet,\bullet)$, $R_h^E(\bullet,\bullet)$ defined as follows:

$$\begin{aligned} S_h^E(v_h, w_h) &:= \sum_{r=1}^{N_E} \mathrm{DOF}_r\Big((\mathrm{Id} - \Pi^{\nabla,E})v_h\Big)\mathrm{DOF}_r\Big((\mathrm{Id} - \Pi^{\nabla,E})w_h\Big), \\ R_h^E(v_h, w_h) &:= |E| \sum_{r=1}^{N_E} \mathrm{DOF}_r\Big((\mathrm{Id} - \Pi^{0,E})v_h\Big)\mathrm{DOF}_r\Big((\mathrm{Id} - \Pi^{0,E})w_h\Big), \end{aligned}$$

where $|E|$ is the area of the polygon E, $N_E := \dim(W_h^E)$ and $\{\mathrm{DOF}_r\}_{r=1}^{N_E}$ denotes the set of local DOFs introduced in Section 3.1.

The global virtual bilinear forms $a_h, m_h : W_h \times W_h \to \mathbb{R}$ are then defined, for all $v_h\, w_h \in W_h^E$, as

$$a_h(v_h, w_h) := \sum_{E\in\mathcal{T}_h} a_h^E(v_h, w_h), \quad m_h(v_h, w_h) := \sum_{E\in\mathcal{T}_h} m_h^E(v_h, w_h).$$

From (3.11) it follows that the global virtual bilinear forms are continuous, namely,

$$\begin{aligned} a_h(v, w) &\lesssim \|\nabla v\|_{L^2(\Omega)}\,\|\nabla w\|_{L^2(\Omega)}, \\ m_h(v, w) &\lesssim \|v\|_{L^2(\Omega)}\,\|w\|_{L^2(\Omega)}. \end{aligned} \tag{3.12}$$

We define the discrete H^1-seminorm and the discrete L^2-norm as follows

$$|\bullet|_{1,h}^2 := a_h(\bullet,\bullet), \quad \|\bullet\|_{0,h}^2 := m_h(\bullet,\bullet). \tag{3.13}$$

Combining (3.11) and (3.12), we find that, for all $v_h, w_h \in W_h$, there holds

$$m_h(v, w) \lesssim \|v_h\|_{0,h}\,\|w_h\|_{0,h}. \tag{3.14}$$

3.3. VE semi-discrete variational problem

We define the VE approximation to the loading term $f(t)$ for all $t \in (0,T)$ as

$$f_h(t)|_E := \Pi^{0,E}f(t) \text{ for all } E \in \mathcal{T}_h,$$

and the VE approximation to the initial conditions u_0, z_0 as the VE interpolants $u_{0,h}$, $z_{0,h}$ of u_0, z_0, specifically, $u_{h,0}$, $z_{h,0}$ are piecewise polynomials of degree less than or equal to k, with evaluations of DOFs coinciding with those of u_0, z_0 (see (3.6)).

The VE semi-discrete approximation to (2.2) reads: find $u_h \in C^0\left(0,T;W_h\right) \cap C^1\left(0,T;W_h\right)$ such that, for all $v_h \in W_h$ and for a.e. $t \in (0,T)$

$$m_h(u_{h,tt}(t), v_h) + \nu m_h(u_{h,t}(t), v_h) + a_h(u_h(t), v_h) = \left(f_h(t), v_h\right)_{L^2(\Omega)}, \tag{3.15}$$

supplemented with the initial conditions $u_h(\cdot,0) = u_{h,0}$, $u_{h,t}(\cdot,0) = z_{h,0}$. By classical arguments, it is possible to show that problem (3.15) admits a unique solution $u_h(t)$ (see Section Appendix A.1). Moreover, there holds the following stability result.

Theorem 3.2. *Let $f_h \in L^2(0,T;L^2(\Omega))$. Then, the unique solution u_h to problem (3.15) fulfills the following inequality, for all $t \in (0,T)$*

$$|u_h(t)|_{1,h}^2 + \|u_{h,t}(t)\|_{0,h}^2 \lesssim |u_{h,0}|_{1,h}^2 + \|z_{h,0}\|_{0,h}^2 + \|f_h\|_{L^2(0,t;L^2(\Omega))}^2. \tag{3.16}$$

Proof. Choosing the test function $v_h = u_{h,t}(t)$ in problem (3.15), and integrating in time between 0 and t, we find

$$\begin{aligned} &\int_0^t m_h(u_{h,tt}(s), u_{h,t}(s))\,\mathrm{d}s + \nu\int_0^t m_h(u_{h,t}(s), u_{h,t}(s))\,\mathrm{d}s \\ &\qquad + \int_0^t a_h(u_h(s), u_{h,t}(s))\,\mathrm{d}s \\ &\quad = \int_0^t \left(f_h(s), u_{h,t}(s)\right)_{L^2(\Omega)}\,\mathrm{d}s. \end{aligned}$$

Observe that

$$\begin{aligned} \int_0^t m_h(u_{h,tt}(s), u_{h,t}(s))\,\mathrm{d}s &= \frac{1}{2}\int_0^t \frac{d}{ds} m_h(u_{h,t}(s), u_{h,t}(s))\,\mathrm{d}s \\ &= \frac{1}{2}\left(\|u_{h,t}(t)\|_{0,h}^2 - \|z_{h,0}\|_{0,h}^2\right), \end{aligned}$$

and, analogously,

$$\begin{aligned} \int_0^t a_h(u_h(s), u_{h,t}(s))\,\mathrm{d}s &= \frac{1}{2}\int_0^t \frac{d}{ds} a_h(u_h(s), u_h(s))\,\mathrm{d}s \\ &= \frac{1}{2}\left(|u_h(t)|_{1,h}^2 - |u_{h,0}|_{1,h}^2\right). \end{aligned}$$

Moreover, using (3.11) we find that

$$\int_0^t m_h(u_{h,t}(s), u_{h,t}(s))\,\mathrm{d}s \gtrsim \int_0^t \|u_{h,t}(s)\|_{L^2(\Omega)}^2\,\mathrm{d}s \gtrsim \|u_{h,t}\|_{L^2(0,t;L^2(\Omega))}^2.$$

Finally, using the Cauchy-Schwarz and Young's inequalities, we find

$$\int_0^t \left(f_h(s), u_{h,t}(s)\right)_{L^2(\Omega)} \, \mathrm{d}s \le \left\|f_h(t)\right\|_{L^2(0,t;L^2(\Omega))} \left\|u_{h,t}\right\|_{L^2(0,t;L^2(\Omega))} \le \frac{1}{2\varepsilon} \left\|f_h(t)\right\|^2_{L^2(0,t;L^2(\Omega))} + \frac{\varepsilon}{2} \left\|u_{h,t}\right\|^2_{L^2(0,t;L^2(\Omega))}.$$

Hence, (3.16) follows for ε sufficiently small. □

Remark 3.3. Let the further assumption $u_h \in H^q(0,T;H^1_0(\Omega))$ for $q \ge 2$ hold, and denote with $\partial_t^q u_h$ the q-th time derivative of u_h (which still fulfills homogeneous Dirichlet boundary conditions on $\partial\Omega$). Then, $w_h := \partial_t^q u_h$ satisfies, for all $v_h \in W_h$ and for a.e. $t \in (0,T)$,

$$m_h(w_{h,tt}(t), v_h) + \nu m_h(w_{h,t}(t), v_h) + a_h(w_h(t), v_h) = \left(\partial_t^q f_h(t), v_h\right)_{L^2(\Omega)},$$

coupled with initial conditions $w_h(0) = w_{h,t}(0) = 0$. Theorem 3.2 then states that

$$\left|w_h(t)\right|^2_{1,h} + \left\|w_{h,t}(t)\right\|^2_{0,h} \lesssim \left\|f_h^{(q)}\right\|^2_{L^2(0,t;L^2(\Omega))}. \tag{3.17}$$

3.4. Error analysis

To perform the error analysis for the semi-discrete problem, we need to introduce the modified energy projection $\mathcal{P}^\nabla : H^1_0(\Omega) \to W_h$, where, for any $u \in H^1_0(\Omega)$, $\mathcal{P}^\nabla u \in W_h$ satisfies, for all $v_h \in W_h$

$$a_h(\mathcal{P}^\nabla u, v_h) = a(u, v_h). \tag{3.18}$$

Similarly, we define the modified L^2-projection $\mathcal{P}^0 : L^2(\Omega) \to W_h$, where, for any $u \in L^2(\Omega)$, $\mathcal{P}^0 u \in W_h$ satisfies, for all $v_h \in W_h$

$$m_h(\mathcal{P}^0 u, v_h) = \left(u, v_h\right)_{L^2(\Omega)}. \tag{3.19}$$

We recall the following approximation results, whose proofs can be found in [5] and [11], respectively.

Lemma 3.4. *For all $u \in H^1_0(\Omega) \cap H^{k+1}(\Omega)$, there holds*

$$\left|u - \mathcal{P}^\nabla u\right|_{H^1(\Omega)} \lesssim h^k \left|u\right|_{H^{k+1}(\Omega)}, \tag{3.20}$$

$$\left\|u - \mathcal{P}^\nabla u\right\|_{L^2(\Omega)} \lesssim h^{k+1} \left|u\right|_{H^{k+1}(\Omega)}. \tag{3.21}$$

Lemma 3.5. *For all $u \in H^{k+1}(\Omega)$, there holds*

$$\left\|u - \mathcal{P}^0 u\right\|_{L^2(\Omega)} \lesssim h^{k+1} \left|u\right|_{H^{k+1}(\Omega)}. \tag{3.22}$$

Let us denote

$$\left|\bullet\right|_{L^1(0,t;H^{k+1}(\Omega))} := \int_0^t \left|\bullet\right|_{H^{k+1}(\Omega)} \, \mathrm{d}s,$$

$$\left|\bullet\right|_{L^2(0,t;H^{k+1}(\Omega))} := \left(\int_0^t \left|\bullet\right|^2_{H^{k+1}(\Omega)} \, \mathrm{d}s\right)^{1/2}.$$

We are now ready to state the following convergence result, which extends [11, Theorem 3.3] to the case $\nu > 0$.

Theorem 3.6. *Let u, u_h be the unique solutions of problems (2.2) and (3.15), respectively. Assume that $u \in C^2\left(0,T;H^1_0(\Omega) \cap H^{k+1}(\Omega)\right)$, u_0, $z_0 \in H^{k+1}(\Omega)$ and u_t, u_{tt}, $f \in L^2\left(0,T;H^{k+1}(\Omega)\right)$, with $k \ge 1$ integer. Then, there holds*

$$\begin{aligned}
&\left\|u_h(t) - u(t)\right\|_{H^1(\Omega)} + \left\|u_{h,t}(t) - u_t(t)\right\|_{L^2(\Omega)} \\
&\lesssim h^k \Big(\left|u_0\right|_{H^{k+1}(\Omega)} + h \left|z_0\right|_{H^{k+1}(\Omega)} + h \left|f\right|_{L^2(0,t;H^{k+1}(\Omega))} \\
&+ \left|u_t\right|_{L^1(0,t;H^{k+1}(\Omega))} + h \left|u_t\right|_{L^2(0,t;H^{k+1}(\Omega))} + h \left|u_{tt}\right|_{L^1(0,t;H^{k+1}(\Omega))} \\
&+ h \left|u_t\right|_{L^2(0,t;H^{k+1}(\Omega))} \Big).
\end{aligned} \tag{3.23}$$

Proof. The proof follows the same steps as the proof of [11, Theorem 3.3]. We set

$$u_h(t) - u(t) = \left(u_h(t) - \mathcal{P}^\nabla u(t)\right) + \left(\mathcal{P}^\nabla u(t) - u(t)\right) =: \theta(t) + \rho(t).$$

We bound the $\left\|\rho(t)\right\|_{H^1(\Omega)}$ by using (3.20)

$$\begin{aligned}
\left\|\rho(t)\right\|_{H^1(\Omega)} &\lesssim h^k \left|u(t)\right|_{H^{k+1}(\Omega)} = h^k \left(\left|u_0\right|_{H^{k+1}(\Omega)} + \int_0^t \left|u_t(s)\right|_{H^{k+1}(\Omega)} \, ds \right) \\
&= h^k \left(\left|u_0\right|_{H^{k+1}(\Omega)} + \left|u_t\right|_{L^1(0,t;H^{k+1}(\Omega))} \right).
\end{aligned} \tag{3.24}$$

Similarly, thanks to (3.21), we find

$$\left\|\rho_t(t)\right\|_{L^2(\Omega)} \lesssim h^{k+1} \left|u_t(t)\right|_{H^{k+1}(\Omega)} = h^{k+1} \left(\left|z_0\right|_{H^{k+1}(\Omega)} + \left|u_{tt}\right|_{L^1(0,t;H^{k+1}(\Omega))} \right). \tag{3.25}$$

Note that we can use the estimate (3.21) since we are assuming Ω convex. In order to bound the norm of $\theta(t)$, we note that, for all $v_h \in W_h$ there holds

$$\begin{aligned}
&m_h(\theta_{tt}(t), v_h) + \nu m_h(\theta_t(t), v_h) + a_h(\theta(t), v_h) \\
&= \left(f_h(t) - f(t), v_h\right)_{L^2(\Omega)} + \left[\left(u_{tt}(t), v_h\right)_{L^2(\Omega)} - m_h(\mathcal{P}^\nabla u_{tt}(t), v_h) \right] \\
&\quad + \nu \left[\left(u_t(t), v_h\right)_{L^2(\Omega)} - m_h(\mathcal{P}^\nabla u_t(t), v_h) \right] \\
&=: \left(\varphi(t), v_h\right)_{L^2(\Omega)} + \left(\eta_1(t), v_h\right)_{L^2(\Omega)} + \left(\eta_2(t), v_h\right)_{L^2(\Omega)},
\end{aligned}$$

where $\eta_1(t), \eta_2(t) \in W_h$ are the Riesz representation of the operators $\left(u_{tt}(t), \bullet\right)_{L^2(\Omega)} - m_h(\mathcal{P}^\nabla u_{tt}(t), \bullet)$ and $\left(u_t(t), \bullet\right)_{L^2(\Omega)} - m_h(\mathcal{P}^\nabla u_t(t), \bullet)$ on the dual space of W_h. Then, $\theta(t)$ is the unique solution of the following weak problem: for all $v_h \in W_h$ there holds

$$\begin{cases}
m_h(\theta_{tt}(t), v_h) + \nu m_h(\theta_t(t), v_h) + a_h(\theta(t), v_h) = \left(\varphi(t) + \eta_1(t) + \eta_2(t), v_h\right)_{L^2(\Omega)} \\
\theta(0) = u_{h,0} - \mathcal{P}^\nabla u_0 \\
\theta_t(0) = z_{h,0} - \mathcal{P}^\nabla z_0.
\end{cases}$$

By applying Theorem 3.2 we find:

$$\begin{aligned}
&\left|\theta(t)\right|^2_{1,h} + \left\|\theta_t(t)\right\|^2_{0,h} \\
&\lesssim \left|\theta_0\right|^2_{1,h} + \left\|\theta_t(0)\right\|^2_{0,h} + \left\|\varphi\right\|^2_{L^2(0,t;L^2(\Omega))} + \left\|\eta_1\right\|^2_{L^2(0,t;L^2(\Omega))} + \left\|\eta_2\right\|^2_{L^2(0,t;L^2(\Omega))}.
\end{aligned} \tag{3.26}$$

On the other hand, using (3.3), we find

$$\begin{aligned}
\left\|\varphi\right\|^2_{L^2(0,t;L^2(\Omega))} &= \int_0^t \left\|\varphi(s)\right\|^2_{L^2(\Omega)} \, \mathrm{d}s = \int_0^t \left\|f_h(s) - f(s)\right\|^2_{L^2(\Omega)} \, \mathrm{d}s \\
&= \int_0^t \sum_{E \in \mathcal{T}_h} \left\|\Pi^{0,E} f(s) - f(s)\right\|^2_{L^2(E)} \, \mathrm{d}s \\
&\lesssim h^{2(k+1)} \left|f\right|^2_{L^2(0,t;H^{k+1}(\Omega))}.
\end{aligned} \tag{3.27}$$

To bound $\left\|\eta_1\right\|^2_{L^2(0,t;L^2(\Omega))}$, we recall [11, equation (32)]: for all $t \in (0,T)$, there holds

$$\left(\eta_1(t), v_h\right)_{L^2(\Omega)} \lesssim h^{k+1} \left|u_{tt}(t)\right|_{H^{k+1}(\Omega)} \left\|v_h\right\|_{L^2(\Omega)},$$

yielding

$$\|\eta_1(t)\|_{L^2(\Omega)} = \sup_{0\neq v_h\in W_h} \frac{\left(\eta_1(t), v_h\right)_{L^2(\Omega)}}{\|v_h\|_{L^2(\Omega)}} \lesssim h^{k+1} |u_{tt}(t)|_{H^{k+1}(\Omega)}.$$

Hence,

$$\|\eta_1\|^2_{L^2(0,t;L^2(\Omega))} = \int_0^t \|\eta_1(s)\|^2_{L^2(\Omega)}\, \mathrm{d}s \lesssim h^{2(k+1)} |u_{tt}|^2_{L^2(0,t;H^{k+1}(\Omega))}. \tag{3.28}$$

Finally, to bound $\|\eta_2\|^2_{L^2(0,t;L^2(\Omega))}$, we observe that, for all $v_h \in W_h$ there holds

$$\begin{aligned}
\left(\eta_2(t), v_h\right)_{L^2(\Omega)} &= \left(u_t(t), v_h\right)_{L^2(\Omega)} - m_h(\mathcal{P}^\nabla u_t(t), v_h) \\
&= \sum_{E\in\mathcal{T}_h} \left[\left(u_t(t), v_h\right)_{L^2(E)} - m_h^E(\mathcal{P}^\nabla u_t(t), v_h)\right] \\
&= \sum_{E\in\mathcal{T}_h} \left[\left(u_t(t) - \Pi^{0,E}u_t(t), v_h\right)_{L^2(E)} - m_h^E(\mathcal{P}^\nabla u_t(t) - \Pi^{0,E}u_t(t), v_h)\right] \\
&\lesssim \sum_{E\in\mathcal{T}_h} \left(\left\|u_t(t) - \Pi^{0,E}u_t(t)\right\|_{L^2(E)} + \left\|\mathcal{P}^\nabla u_t(t) - \Pi^{0,E}u_t(t)\right\|_{L^2(E)}\right) \|v_h\|_{L^2(E)},
\end{aligned}$$

where in the third equality we used that $\left(\Pi^{0,E}u_t(t), v_h\right)_{L^2(E)} = m_h^E(\Pi^{0,E}u_t(t), v_h)$, and the last inequality follows by the Cauchy Schwarz inequality and (3.12). Hence, by using (3.3) and applying Lemma 3.4, we obtain

$$\|\eta_2(t)\|_{L^2(\Omega)} = \sup_{0\neq v_h\in W_h} \frac{\left(\eta_1(t), v_h\right)_{L^2(\Omega)}}{\|v_h\|_{L^2(\Omega)}} \lesssim h^{k+1} |u_t(t)|_{H^{k+1}(\Omega)},$$

hence

$$|\eta_2|^2_{L^2(0,t;L^2(\Omega))} \lesssim h^{2(k+1)} |u_t|^2_{L^2(0,t;H^{k+1}(\Omega))}. \tag{3.29}$$

The norm of the initial data is derived in [11, equations (33)-(34)]:

$$\begin{aligned}
|\theta_0|^2_{1,h} &\lesssim h^{2k} |u_0|^2_{H^{k+1}(\Omega)}, \\
\|\theta_t(0)\|^2_{0,h} &\lesssim h^{2(k+1)} |z_0|^2_{H^{k+1}(\Omega)}.
\end{aligned} \tag{3.30}$$

Combining (3.30), (3.27), (3.28) and (3.29), we obtain

$$\begin{aligned}
|\theta(t)|^2_{1,h} + \|\theta_t(t)\|^2_{0,h} \lesssim h^{2k}\Big[&|u_0|^2_{H^{k+1}(\Omega)} + h^2 |z_0|^2_{H^{k+1}(\Omega)} \\
&+ h^2\big(|f|^2_{L^2(0,t;H^{k+1}(\Omega))} + |u_{tt}|^2_{L^2(0,t;H^{k+1}(\Omega))} + |u_t|^2_{L^2(0,t;H^{k+1}(\Omega))}\big)\Big].
\end{aligned} \tag{3.31}$$

Collecting (3.24), (3.25) and (3.31), we conclude (3.23). □

3.5. Algebraic formulation

Now, we introduce the algebraic formulation of (3.15) that will be instrumental for the DG discretization in time (see Section 4). To this end, we denote with $N_h := \dim(W_h)$, and with $\{\varphi_i\}_{i=1}^{N_h}$ the set of VE basis functions for W_h. We write, for all $t \in (0,T)$

$$u_h(t,x) = \sum_{j=1}^{N_h} U_j(t)\varphi_j(x), \tag{3.32}$$

where $U_j(t)$ is the j-th global DOF of $u_h(t)$. Inserting (3.32) into (3.15) with $v_h = \varphi_i$, we obtain the following system of second-order differential equations

$$M_h\ddot{\mathbf{U}}(t) + \nu M_h\dot{\mathbf{U}}(t) + A_h\mathbf{U}(t) = \mathbf{F}_h(t) \tag{3.33}$$

where

- $\mathbf{U}(t) := [U_1(t), \dots, U_{N_h}(t)]^T \in \mathbb{R}^{N_h}$;
- $\dot{\mathbf{U}}(t) := [\dot{U}_1(t), \dots, \dot{U}_{N_h}(t)]^T \in \mathbb{R}^{N_h}$ is the vector collecting the DOF of the first temporal derivative of u, i.e., $u_{h,t}(t,x) = \sum_{j=1}^{N_h} \dot{U}_j(t)\varphi_j(x)$;
- $\ddot{\mathbf{U}}(t) := [\ddot{U}_1(t), \dots, \ddot{U}_{N_h}(t)]^T \in \mathbb{R}^{N_h}$ is the vector collecting the DOF of the second temporal derivative of u, i.e., $u_{h,tt}(t,x) = \sum_{j=1}^{N_h} \ddot{U}_j(t)\varphi_j(x)$;
- $\mathbf{F}_h(t) := [F_1(t), \dots, F_{N_h}(t)]^T \in \mathbb{R}^{N_h}$ with $F_i(t) := \left(f_h(t), \varphi_i\right)_{L^2(\Omega)}$ for all $i = 1, \dots, N_h$;
- M_h, $A_h \in \mathbb{R}^{N_h\times N_h}$ are the mass and stiffness matrices with elements given as

$$\text{for all } i,j = 1, \dots, N_h \quad (M_h)_{i,j} := m_h(\varphi_j, \varphi_i) \quad (A_h)_{i,j} := a_h(\varphi_j, \varphi_i). \tag{3.34}$$

Equation (3.33) is supplemented with the initial conditions $\mathbf{U}(0) = \mathbf{U}_{h,0}$, $\dot{\mathbf{U}}(0) = \mathbf{Z}_{h,0}$, where the vector $\mathbf{U}_{h,0} \in \mathbb{R}^{N_h}$ ($\mathbf{Z}_{h,0} \in \mathbb{R}^{N_h}$, respectively) collects the DOFs of $u_{h,0}$ ($z_{h,0}$, respectively).

4. DG discretization in time

In this section we first recall the DG (in time) finite dimensional space introduced in [49,21], and then we apply the DG time integration scheme to (3.33). Let the time interval $(0,T]$ be partitioned into N_T time-slabs, i.e., $(0,T] = \cup_{n=1}^{N_T} I_n$, with $I_n := (t_{n-1}, t_n]$ and $0 = t_0 < t_1 < \cdots < t_n < \cdots < t_{N_T} = T$. We denote with τ_n the length of the n-th time-slab $\tau_n := t_n - t_{n-1}$, and we collect the elements of the set $\{\tau_n\}_{n=1}^{N_T}$ in the vector $\boldsymbol{\tau}$. Moreover, we denote with $\mathcal{I}_{\boldsymbol{\tau}}$ the partition of the time interval. Given a sufficiently regular function v, we define the time jump operator at t_n for any $n \geq 0$ as

$$[v]_n := v(t_n^+) - v(t_n^-), \tag{4.1}$$

where

$$v(t_n^+) = \lim_{\varepsilon\to 0^+} v(t_n + \varepsilon), \quad v(t_n^-) = \lim_{\varepsilon\to 0^-} v(t_n + \varepsilon).$$

See Fig. 4.1 for an example of time partition as well as the graphical representation of t_{n-1}^-, t_{n-1}^+.

Given $r_n \in \mathbb{N}$, we denote the space of polynomials on I_n of degree less than or equal to r_n as $\mathbb{P}_{r_n}(I_n)$, and we define the functional space of piecewise polynomials of degree at least 2 on $\mathcal{I}_{\boldsymbol{\tau}}$ as

$$\begin{aligned}
W_{\boldsymbol{\tau}} := \Big\{ &v \in L^2(0,T) \text{ such that } v|_{I_n} \in \mathbb{P}_{r_n}(I_n) \\
&\text{with } r_n \geq 2 \text{ for all } n = 1, \dots, N_T \Big\}.
\end{aligned} \tag{4.2}$$

Note that the choice $r_n \geq 2$ is due to the presence of the second order time derivative in the equation at hand.

Since the unknown of (3.33) is a vector with length N_h, we need to introduce the multi-variate version of $W_{\boldsymbol{\tau}}$. Given the multi-index $\mathbf{r} = (r_1, \dots, r_{N_\tau}) \in \mathbb{N}^{N_T}$, with components $r_n \geq 2$ for all $n = 1, \dots, N_T$, we define

$$[W_{\boldsymbol{\tau}}]^{N_h} := \left\{ \mathbf{V} = (v_1, \dots, v_{N_h}) \in [L^2(0,T)]^{N_h} : v_j \in W_{\boldsymbol{\tau}}\ \forall j = 1, \dots, N_h \right\}.$$

Multiplying (3.33) by a test function $\dot{\mathbf{V}} \in [W_{\boldsymbol{\tau}}]^{N_h}$ and integrating on I_n, we get

$$\begin{aligned}
&\left(M_h\ddot{\mathbf{U}}, \dot{\mathbf{V}}\right)_{L^2(I_n)} + \nu\left(M_h\dot{\mathbf{U}}, \dot{\mathbf{V}}\right)_{L^2(I_n)} + \left(A_h\mathbf{U}, \dot{\mathbf{V}}\right)_{L^2(I_n)} \\
&\quad + M_h[\dot{\mathbf{U}}]_n \cdot \dot{\mathbf{V}}(t_n^+) + A_h[\mathbf{U}]_n \cdot \mathbf{V}(t_n^+) = \left(\mathbf{F}_h, \dot{\mathbf{V}}\right)_{L^2(I_n)}
\end{aligned} \tag{4.3}$$

where the first two terms in the second row of (4.3) are zero since $\mathbf{U}(t) \in C^2(0,T)$, hence they can be added to the equation. Summing over all time-slabs, we find the following problem: find $\mathbf{U}_{\boldsymbol{\tau}} \in [W_{\boldsymbol{\tau}}]^{N_h}$ such that, for all $\dot{\mathbf{V}} \in [W_{\boldsymbol{\tau}}]^{N_h}$ there holds

$$\begin{aligned}
&\sum_{n=1}^{N_T} \left[\left(M_h\ddot{\mathbf{U}}_{\boldsymbol{\tau}}, \dot{\mathbf{V}}\right)_{L^2(I_n)} + \nu\left(M_h\dot{\mathbf{U}}_{\boldsymbol{\tau}}, \dot{\mathbf{V}}\right)_{L^2(I_n)} + \left(A_h\mathbf{U}_{\boldsymbol{\tau}}, \dot{\mathbf{V}}\right)_{L^2(I_n)}\right] \\
&\quad + \sum_{n=1}^{N_T-1} \left[M_h[\dot{\mathbf{U}}_{\boldsymbol{\tau}}]_n \cdot \dot{\mathbf{V}}(t_n^+) + A_h[\mathbf{U}_{\boldsymbol{\tau}}]_n \cdot \mathbf{V}(t_n^+)\right] \\
&\quad + M_h\dot{\mathbf{U}}_{\boldsymbol{\tau}}(0^+) \cdot \dot{\mathbf{V}}(0^+) + A_h\mathbf{U}_{\boldsymbol{\tau}}(0^+) \cdot \mathbf{V}(0^+) \\
&\quad = \sum_{n=1}^{N_T} \left[\left(\mathbf{F}_h, \dot{\mathbf{V}}\right)_{L^2(I_n)}\right] + M_h\mathbf{Z}_{h,0} \cdot \dot{\mathbf{V}}(0^+) + A_h\mathbf{U}_{h,0} \cdot \mathbf{V}(0^+),
\end{aligned} \tag{4.4}$$

with the initial conditions $\mathbf{U}_{\boldsymbol{\tau}}(0) = \mathbf{U}_{h,0}$, $\dot{\mathbf{U}}_{\boldsymbol{\tau}}(0) = \mathbf{Z}_{h,0}$.

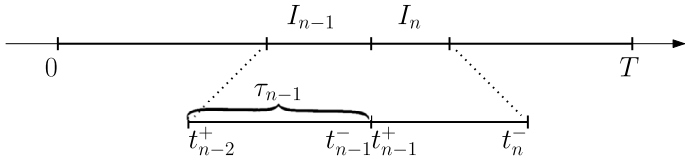

Fig. 4.1. (Top) Example of time partition $\mathcal{I}_\tau$. (Bottom) Zoom on the time-slabs $I_{n-1} \cup I_n$.

Let $\|\bullet\|_\star : [W_\tau]^{N_h} \to \mathbb{R}$ be defined as

$$\begin{aligned}\|\mathbf{V}\|_\star^2 := \nu \sum_{n=1}^{N_T} \left\| M_h^{1/2} \dot{\mathbf{V}} \right\|^2_{L^2(I_n)} \\ + \frac{1}{2}(M_h^{1/2}\dot{\mathbf{V}}(0^+))^2 + \frac{1}{2}\sum_{n=1}^{N_T-1}(M_h^{1/2}[\dot{\mathbf{V}}]_n)^2 + \frac{1}{2}(M_h^{1/2}\dot{\mathbf{V}}(T^-))^2 \\ + \frac{1}{2}(A_h^{1/2}\mathbf{V}(0^+))^2 + \frac{1}{2}\sum_{n=1}^{N_T-1}(A_h^{1/2}[\mathbf{V}]_n)^2 + \frac{1}{2}(A_h^{1/2}\mathbf{V}(T^-))^2.\end{aligned} \tag{4.5}$$

In [21] it is shown that $\|\bullet\|_\star$ is a norm on $[W_\tau]^{N_h}$ that, from now on, will be referred to as energy norm.

Moreover, in [49, Proposition 3.1] it is proved the following stability result: if $\mathbf{F} \in L^2(0,T)$, then the unique solution $\mathbf{U}_\tau \in [W_\tau^{\mathbf{r}}]^{N_h}$ of (4.4) satisfies

$$\|\mathbf{U}_\tau\|_\star \lesssim \left(\|\mathbf{F}\|^2_{L^2(0,T)} + (A_h^{1/2}\mathbf{U}_{h,0})^2 + (M_h^{1/2}\mathbf{Z}_{h,0})^2 \right)^{1/2}. \tag{4.6}$$

In addition, the DG scheme is proved to be convergent, according to the following result (see [49, Theorem 3.12]).

Theorem 4.1. *If* $\mathbf{U}$ *is such that* $\mathbf{U}|_{I_n} \in \left(H^{q_n}(I_n)\right)^{N_h}$ *with* $q_n \geq 2$ *for all* $n = 1, \dots, N_T$, *then*

$$\|\mathbf{U} - \mathbf{U}_\tau\|_\star^2 \lesssim \sum_{n=1}^{N_T} \frac{\tau_n^{2\beta_n - 3}}{r_n^{2q_n-6}} \|\mathbf{U}\|^2_{(H^{q_n}(I_n))^{N_h}}, \tag{4.7}$$

where $\beta_n := \min\{r_n + 1, q_n\}$ *and* $r_n \geq 2$ *for all* $n = 1, \dots, N_T$.

Corollary 4.2. *Let* $\mathbf{U}$ *be such that* $\mathbf{U}|_{I_n} \in \left(H^q(I_n)\right)^{N_h}$ *for all* $n = 1, \dots, N_T$, *with* $q \geq 2$. *Moreover, let* $\tau_n = \Delta t > 0$ *and* $r_n = r \geq 2$ *integer, for all* $n = 1, \dots, N_T$. *Then, the estimate* (4.7) *simplifies as follows:*

$$\|\mathbf{U} - \mathbf{U}_\tau\|_\star^2 \lesssim \frac{\Delta t^{2\beta-3}}{r^{2q-6}} \sum_{n=1}^{N_T} \|\mathbf{U}\|^2_{(H^{q_n}(I_n))^{N_h}}, \tag{4.8}$$

where $\beta := \min\{r+1, q\}$. *In particular,* $\|\mathbf{U} - \mathbf{U}_\tau\|_\star = O(\Delta t^{\beta - 3/2})$ *as* Δt *decreases to 0.*

Remark 4.3. The presented DG method is computationally more expensive than standard "finite difference" time-stepping methods, like, e.g., Newmark or leap-frog method, which are typically simpler and faster to be implemented. On the other hand, it is worth noticing that it presents a few important advantages. First of all, it is of arbitrarily high order, in contrast to standard time-stepping methods that are low-order schemes (Newmark, e.g., is second order accurate). Moreover, it is unconditionally stable, in contrast to Newmark scheme, which is unconditionally stable for appropriate choices of the parameters only.

5. VEM-DG discretization

In this section we present a tensor product-based space-time discretization of problem (2.2) that combines the VEM presented in Section 3 for space discretization, with the DG scheme presented in Section 4 for time integration. The mesh $\mathcal{Q}$ for the space-time domain $\Omega \times (0,T]$ is constructed by tensorizing the polygonal grid $\mathcal{T}_h$ with the time interval partition $\mathcal{I}_\tau$, namely, $\mathcal{Q} := \mathcal{T}_h \otimes \mathcal{I}_\tau$. Each element of the space-time mesh $\mathcal{Q}$ is the tensor product of the polygonal mesh $\mathcal{T}_h$ with I_n, i.e.,

$$\mathcal{Q} = \cup_{n=1}^{N_T} Q_n, \text{with } Q_n := \mathcal{T}_h \otimes I_n \text{ for all } n = 1, \dots, N_T. \tag{5.1}$$

We refer to Fig. 5.1 for an example.

The tensor product of the VE space W_h defined in (3.5) with the DG space W_τ defined in (4.2) gives the following finite-dimensional space

$$\begin{aligned}\mathcal{W}_{h,\tau} := \big\{ w(x,t) = w_1(x)w_2(t) : \Omega \times (0,T] \to \mathbb{R} \text{ such that } w_1 \in W_h \\ \text{and } w_2 \in W_\tau \big\}.\end{aligned} \tag{5.2}$$

Note that, by definition, each $w \in \mathcal{W}_{h,\tau}$ is continuous in the spatial domain but might be discontinuous in the time domain, i.e., discontinuities are allowed along the interfaces $\mathcal{T}_h \otimes \{t_n\}$, for $n = 1, \dots, N_T - 1$.

To derive the tensor product VEM-DG formulation of the problem of interest, we start from equation (2.1) in Q_n multiplied by a test function $\dot{w} = w_1(x)\dot{w}_2(t) \in \mathcal{W}_{h,\tau}$ and we integrate in space and time. Then, we integrate by parts with respect to the space variable and we replace the $L^2(\Omega)$-inner product $(\bullet,\bullet)_{L^2(\Omega)}$ and the bilinear form $a(\bullet,\bullet)$ with the VE bilinear forms $m_h(\bullet,\bullet)$ and $a_h(\bullet,\bullet)$, respectively. Finally, we add the null terms

$$m_h([\dot{u}]_n, \dot{w}(t_n^+)) + a_h([u]_n, \dot{w}(t_n^+))$$

and we sum up over all time-slabs. As a result, we get the following problem: find $u_{h,\tau} \in \mathcal{W}_{h,\tau}$ such that, for all $w \in \mathcal{W}_{h,\tau}$ there holds

$$\mathcal{A}(u_{h,\tau}, w) = \mathcal{F}(w), \tag{5.3}$$

where the bilinear form $\mathcal{A} : \mathcal{W}_{h,\tau} \times \mathcal{W}_{h,\tau} \to \mathbb{R}$ and the linear form $\mathcal{F} : \mathcal{W}_{h,\tau} \to \mathbb{R}$ are respectively given by

$$\begin{aligned}\mathcal{A}(v,w) := \sum_{n=1}^{N_T} \Big[m_h(v_1,w_1)\left(\ddot{v}_2, \dot{w}_2\right)_{L^2(I_n)} + \nu m_h(v_1,w_1)\left(\dot{v}_2, \dot{w}_2\right)_{L^2(I_n)} \\ + a_h(v_1,w_1)\left(v_2, \dot{w}_2\right)_{L^2(I_n)} \Big] \\ + \sum_{n=1}^{N_T-1} \Big[m_h(v_1,w_1)[\dot{v}_2]_n \dot{w}_2(t_n^+) + a_h(v_1,w_1)[v_2]_n w_2(t_n^+) \Big] \\ + m_h(v_1,w_1)\dot{v}_2(0^+)\dot{w}_2(0^+) + a_h(v_1,w_1)v_2(0^+)w_2(0^+),\end{aligned}$$

and

$$\mathcal{F}(w) := \sum_{n=1}^{N_T} (f_h, w)_{L^2(\Omega \times I_n)} + m_h(z_{h,0}, w_1)\dot{w}_2(0^+) + a_h(u_{h,0}, w_1)w_2(0^+),$$

for any $v(x,t) = v_1(x)v_2(t)$ and $w(x,t) = w_1(x)w_2(t)$.

There holds the following results.

Lemma 5.1. *The function* $|||\bullet||| : H^2(0,T; H_0^1(\Omega)) \to \mathbb{R}$ *defined as*

$$\begin{aligned}|||w|||^2 := \nu \sum_{n=1}^{N_T} \int_{I_n} \|\dot{w}\|^2_{0,h}\, dt \\ + \frac{1}{2}\|\dot{w}(0^+,\cdot)\|^2_{0,h} + \frac{1}{2}\sum_{n=1}^{N_T-1} \|[\dot{w}]_n\|^2_{0,h} + \frac{1}{2}\|\dot{w}(T^-,\cdot)\|^2_{0,h} \\ + \frac{1}{2}|w(0^+,\cdot)|^2_{1,h} + \frac{1}{2}\sum_{n=1}^{N_T-1} |[w]_n|^2_{1,h} + \frac{1}{2}|w(T^-,\cdot)|^2_{1,h}\end{aligned} \tag{5.4}$$

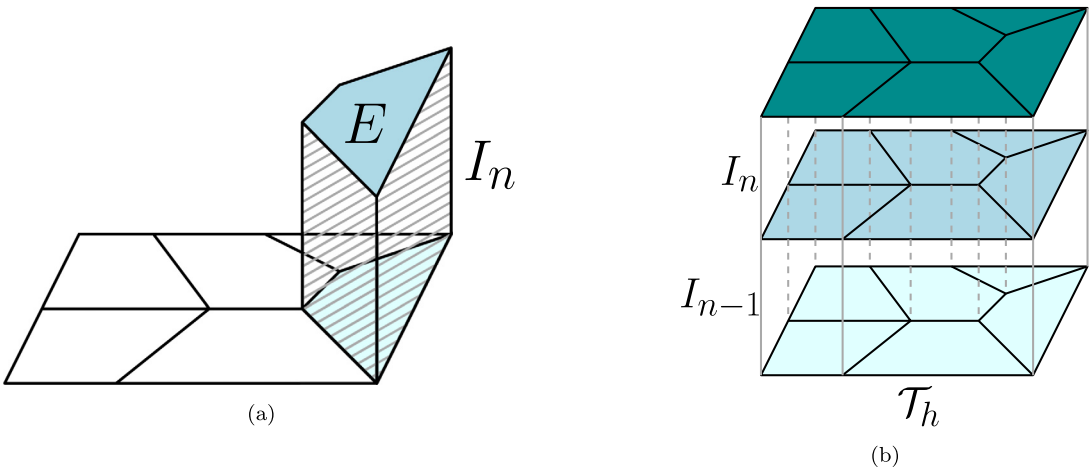

Fig. 5.1. (a) Polygon $E \in \mathcal{T}_h$ tensorized with the time-slab I_n. (b) Polygonal mesh $\mathcal{T}_h$ tensorized with $I_{n-1} \cup I_n$, namely, $Q_{n-1} \cup Q_n$. Darker color encodes the increasing time instances.

is a norm on $H^2(0,T;H^1_0(\Omega))$.

Proof. It is clear that the function $|||\bullet|||$ satisfies the homogeneity and subadditivity properties. Moreover, if $w = 0$, then it immediately follows that $|||w||| = 0$. Therefore, $|||\bullet|||$ is a seminorm on $H^2(0,T;H^1_0(\Omega))$. We show that $|||w||| = 0$ implies $w = 0$ following the same steps as in the proof of [21, Proposition 2].

The fact that $|||w||| = 0$ implies that all the terms at the right-hand side of (5.4) are zero. In particular, for all $n = 1, \dots, N_T$, there holds

$$\int_{I_n} \|\dot{w}\|^2_{0,h} \, \mathrm{d}t = 0,$$

which, in turns, implies $\dot{w} \equiv 0$ in $\Omega \times I_n$, that is, $w \equiv C_n$ in $\Omega \times I_n$ for $\{C_n\}_{n=1}^{N_T}$ a collection of constants. For $n = 1$, we have $w \equiv C_1$ in $\Omega \times I_1$. In addition, from

$$\|w(0^+,\cdot)\|_{0,h} = 0,$$

we get $w(0^+,\cdot) \equiv 0$ in Ω. Hence, we conclude $C_1 = 0$, i.e., $w \equiv 0$ in $\Omega \times I_1$.

We proceed now by induction, namely, we assume $w \equiv 0$ in all $\Omega \times I_m$ for $m \le n-1$, and we show that $w \equiv 0$ in $\Omega \times I_n$. From

$$|[w]_{n-1}|_{1,h} = 0$$

we get $[w]_{n-1} = 0$, i.e., $w(t^+_{n-1},x) = w(t^-_{n-1},x)$ for a.e. $x \in \Omega$. Since $w(t^-_{n-1},\cdot) \equiv 0$ in Ω by assumption, we get $w(t^+_{n-1},\cdot) \equiv 0$ in Ω, which in turns implies $C_n = 0$. □

Lemma 5.2. *For all* $w(x,t) = w_1(x)w_2(t) \in \mathcal{W}_{h,\boldsymbol{\tau}}$ *there holds*

$$|||w|||^2 = \mathcal{A}(w,w). \tag{5.5}$$

Proof. Given $w(x,t) = w_1(x)w_2(t) \in \mathcal{W}_{h,\boldsymbol{\tau}}$, we have

$$\begin{aligned}\mathcal{A}(w,w) := \sum_{n=1}^{N_T} \Big[&\|w_1\|^2_{0,h} \left(\ddot{w}_2, \dot{w}_2\right)_{L^2(I_n)} + \nu \|w_1\|^2_{0,h} \|\dot{w}_2\|^2_{L^2(I_n)} \\ &+ |w_1|^2_{1,h} \left(w_2, \dot{w}_2\right)_{L^2(I_n)} \Big] \\ &+ \sum_{n=1}^{N_T-1} \left[\|w_1\|^2_{0,h} [\dot{w}_2]_n \dot{w}_2(t^+_n) + |w_1|^2_{1,h} [v_2]_n w_2(t^+_n) \right] \\ &+ \|w_1\|^2_{0,h} \left(\dot{w}_2(0^+)\right)^2 + |w_1|^2_{1,h} \left(w_2(0^+)\right)^2 .\end{aligned} \tag{5.6}$$

Integrating by parts, we get

$$\left(\ddot{w}_2, \dot{w}_2\right)_{L^2(I_n)} = -\left(\dot{w}_2, \ddot{w}_2\right)_{L^2(I_n)} + \left(\dot{w}_2(t^-_n)\right)^2 - \left(\dot{w}_2(t^+_{n-1})\right)^2,$$

which implies

$$\left(\ddot{w}_2, \dot{w}_2\right)_{L^2(I_n)} = \frac{1}{2}\left(\dot{w}_2(t^-_n)\right)^2 - \frac{1}{2}\left(\dot{w}_2(t^+_{n-1})\right)^2. \tag{5.7}$$

Analogously, we derive

$$\left(\dot{w}_2, w_2\right)_{L^2(I_n)} = \frac{1}{2}\left(w_2(t^-_n)\right)^2 - \frac{1}{2}\left(w_2(t^+_{n-1})\right)^2. \tag{5.8}$$

Inserting (5.7) and (5.8) into (5.6), and performing simple computations, we derive

$$\begin{aligned}\mathcal{A}(w,w) = \nu \|w_1\|^2_{0,h} \sum_{n=1}^{N_T} \|\dot{w}_2\|^2_{L^2(I_n)} &+ \frac{1}{2}\|w_1\|^2_{0,h} \left[\left(\dot{w}_2(0^+)\right)^2 + \sum_{n=1}^{N_T-1} \left([\dot{w}_2]_n\right)^2 + \left(\dot{w}_2(T^-)\right)^2 \right] \\ &+ \frac{1}{2}|w_1|^2_{1,h} \left[\left(w_2(0^+)\right)^2 + \sum_{n=1}^{N_T-1} \left([w_2]_n\right)^2 + \left(w_2(T^-)\right)^2 \right]\end{aligned}$$

and we conclude by observing that

$$\|w_1\|^2_{0,h} \sum_{n=1}^{N_T} \|\dot{w}_2\|^2_{L^2(I_n)} = \sum_{n=1}^{N_T} \int_{I_n} m_h(\dot{w},\dot{w}) \, \mathrm{d}t = \sum_{n=1}^{N_T} \int_{I_n} \|\dot{w}\|^2_{0,h} \, \mathrm{d}t,$$

and

$$\begin{aligned}\|w_1\|^2_{0,h} \left(\dot{w}_2(0^+)\right)^2 &= \|\dot{w}(0^+,\cdot)\|^2_{0,h} \\ \|w_1\|^2_{0,h} \left([\dot{w}_2]_n\right)^2 &= \|[\dot{w}]_n\|^2_{0,h} \\ \|w_1\|^2_{0,h} \left(\dot{w}_2(T^-)\right)^2 &= \|\dot{w}(T^-,\cdot)\|^2_{0,h}\end{aligned}$$

as well as

$$\begin{aligned}|w_1|^2_{1,h} \left(w_2(0^+)\right)^2 &= \|w(0^+,\cdot)\|^2_{0,h} \\ |w_1|^2_{1,h} \left([w_2]_n\right)^2 &= \|[w]_n\|^2_{0,h} \\ |w_1|^2_{1,h} \left(w_2(T^-)\right)^2 &= \|w(T^-,\cdot)\|^2_{0,h}.\end{aligned}$$

□

Theorem 5.3 *(Well-posedness). There exists a unique solution to the VEM-DG problem* (5.3).

Proof. Lemma 5.2 implies that the bilinear form $\mathcal{A}(\bullet,\bullet)$ is coercive, with coercivity constant 1. The continuity of $\mathcal{F}$ follows from Cauchy-Schwarz inequality and the continuity of the global virtual bilinear forms (3.12). □

5.1. Algebraic formulation

In this section we derive the algebraic formulation of the fully discrete problem (5.3). We start noticing that the use of DG in time allows us to compute the discrete solution separately, one time-slab at a time. In particular, given $1 \le n \le N_T$, problem (5.3) restricted to I_n reads: find $u^n_{h,\boldsymbol{\tau}} := u_{h,\boldsymbol{\tau}}|_{I_n} \in W_h \otimes \mathbb{P}_{r_n}(I_n)$ such that, for all $w \in W_h \otimes \mathbb{P}_{r_n}(I_n)$ there holds

$$\mathcal{A}_n(u^n_{h,\boldsymbol{\tau}}, w) = \mathcal{F}_n(w), \tag{5.9}$$

where

$$\begin{aligned}\mathcal{A}_n(v,w) :=\ & m_h(v_1,w_1)\left(\ddot{v}_2,\dot{w}_2\right)_{L^2(I_n)} + \nu m_h(v_1,w_1)\left(\dot{v}_2,\dot{w}_2\right)_{L^2(I_n)} \\ & + a_h(v_1,w_1)\left(v_2,\dot{w}_2\right)_{L^2(I_n)} + m_h(v_1,w_1)\dot{v}_2(t^+_{n-1})\dot{w}_2(t^+_{n-1}) \\ & + a_h(v_1,w_1)v_2(t^+_{n-1})w_2(t^+_{n-1}),\end{aligned}$$

and

$$\begin{aligned}\mathcal{F}_n(w) :=\ & (f_h,w)_{L^2(\Omega\times I_n)} + m_h(\dot{u}^{n-1}_{h,\boldsymbol{\tau}}(t^-_{n-1},\cdot),\dot{w}(t^-_{n-1},\cdot) \\ & + a_h(u^{n-1}_{h,\boldsymbol{\tau}}(t^-_{n-1},\cdot),w(t^-_{n-1},\cdot),\end{aligned}$$

for any $v(x,t) = v_1(x)v_2(t) \in W_h \otimes \mathbb{P}_{r_n}(I_n)$ and $w(x,t) = w_1(x)w_2(t) \in W_h \otimes \mathbb{P}_{r_n}(I_n)$. Note, in particular, that the solution computed for I_{n-1} is used as initial condition for the current time-slab.

Following the same notation as in Section 3.5, we write $W_h = span\{\varphi_j\}_{j=1}^{N_h}$. Moreover, we denote with $\{\psi_m\}_{m=1}^{r_n}$ a basis for $\mathbb{P}_{r_n}(I_n)$. In the numerical examples, we take Lagrange basis functions with Legendre-Gauss-Lobatto nodes [56]. Then, the trial function $u^n_{h,\boldsymbol{\tau}}$ can be expressed as linear combination of the tensor product basis function $\{\varphi_j\phi_m,\ j=1,\dots,N_h,\ m=1,\dots,r_n+1\}$, namely

$$u^n_{h,\boldsymbol{\tau}}(x,t) = \sum_{j=1}^{N_h}\sum_{m=1}^{r_n+1} \alpha^n_{j,m}\varphi_j(x)\psi_m(t), \tag{5.10}$$

where $\alpha^n_{j,m} \in \mathbb{R}$ for all $j=1,\dots,N_h$, $m=1,\dots,r_n+1$. Inserting (5.10) into (5.9) and taking $w(x,t) = \varphi_i(x)\psi_\ell(t)$, we get

$$A^n\boldsymbol{\alpha}^n = \mathbf{F}^n,$$

where

- $\boldsymbol{\alpha}^n \in \mathbb{R}^{N_h(r_n+1)}$ is the solution vector;
- $A^n \in \mathbb{R}^{N_h(r_n+1)\times N_h(r_n+1)}$ has the following structure:

  $$A^n = M_h \otimes (N_1 + \nu N_2 + N_4) + A_h \otimes (N_3 + N_5),$$

  where M_h, $A_h \in \mathbb{R}^{N_h\times N_h}$ are the mass and stiffness matrices defined in (3.34), and N_1, N_2, N_3, N_4, $N_5 \in \mathbb{R}^{(r_n+1)\times(r_n+1)}$ are defined as

  $$(N_1)_{\ell,m} = (\ddot{\psi}_m,\dot{\psi}_\ell)_{L^2(I_n)}, \quad (N_2)_{\ell,m} = (\dot{\psi}_m,\dot{\psi}_\ell)_{L^2(I_n)},$$
  $$(N_3)_{\ell,m} = (\psi_m,\dot{\psi}_\ell)_{L^2(I_n)}, \quad (N_4)_{\ell,m} = \dot{\psi}_m(t^+_{n-1})\dot{\psi}_\ell(t^+_{n-1}),$$
  $$(N_5)_{\ell,m} = \psi_m(t^+_{n-1})\psi_\ell(t^+_{n-1});$$

- $\mathbf{F}^n \in \mathbb{R}^{N_h(r_n+1)}$ is the known vector with elements

  $$(\mathbf{F}^n)_{i,\ell} = (f_h,\varphi_i\psi_\ell)_{L^2(\Omega\times I_n)} + (M_h\otimes N_6)\boldsymbol{\alpha}^{n-1} + (A_h\otimes N_7)\boldsymbol{\alpha}^{n-1},$$

  where N_6, $N_7 \in \mathbb{R}^{(r_n+1)\times(r_n+1)}$ are defined as

  $$(N_6)_{\ell,m} = \dot{\psi}_m(t^-_{n-1})\dot{\psi}_\ell(t^-_{n-1}), \quad (N_7)_{\ell,m} = \psi_m(t^-_{n-1})\psi_\ell(t^-_{n-1}).$$

6. Error analysis

Before stating the convergence result for the tensor product VEM-DG method, we introduce the following auxiliary lemma.

Lemma 6.1. *Let $u_{h,\boldsymbol{\tau}} \in \mathcal{W}_{h,\boldsymbol{\tau}}$ and $\mathbf{U} \in [W_{\boldsymbol{\tau}}]^{N_h}$ be the solutions of problems (5.3) and (4.4), respectively. Then,*

$$|||u_{h,\boldsymbol{\tau}}||| = \|\mathbf{U}\|_\star.$$

Proof. We follow the same reasoning as in [21, Proposition 3]. We write $u_{h,\boldsymbol{\tau}}(x,t) = u_1(x)u_2(t)$, with $u_2 \in W_{\boldsymbol{\tau}}$ and $u_1(x) = \sum_{j=1}^{N_h} U_j\varphi_j(x)$, $\{\varphi_j\}_{j=1}^{N_h}$ being the VE basis functions. We set $\mathbf{U}(t) = [U_1,\dots,U_{N_h}]^T w_2(t) \in [W_{\boldsymbol{\tau}}]^{N_h}$. By definition (5.4), we have

$$\begin{aligned}|||u_{h,\boldsymbol{\tau}}|||^2 =\ & \nu\sum_{n=1}^{N_T}\int_{I_n}\|\dot{w}\|^2_{0,h}\,\mathrm{d}t \\ & + \frac{1}{2}\|u^+_{h,\boldsymbol{\tau}}(0^+,\cdot)\|^2_{0,h} + \frac{1}{2}\sum_{n=1}^{N_T-1}\|[u_{h,\boldsymbol{\tau}}]_n\|^2_{0,h} + \frac{1}{2}\|u^-_{h,\boldsymbol{\tau}}(T^-,\cdot)\|^2_{0,h} \\ & + \frac{1}{2}|u_{h,\boldsymbol{\tau}}(0^+,\cdot)|^2_{1,h} + \frac{1}{2}\sum_{n=1}^{N_T-1}|[u_{h,\boldsymbol{\tau}}]_n|^2_{1,h} + \frac{1}{2}|u_{h,\boldsymbol{\tau}}(T^-,\cdot)|^2_{1,h}.\end{aligned} \tag{6.1}$$

We observe that

$$\begin{aligned}\int_{I_n}\|\dot{w}\|^2_{0,h}\,\mathrm{d}t &= \int_{I_n}\sum_{i,j=1}^{N_h}\left(U_iu_2(t)\right)(M_h)_{i,j}\left(U_ju_2(t)\right)\,\mathrm{d}t \\ &= \int_{I_n}\mathbf{U}(t)^T M_h\mathbf{U}(t)\,\mathrm{d}t = \left\|M_h^{1/2}\mathbf{U}\right\|^2_{L^2(I_n)}.\end{aligned}$$

Hence, $\sum_{n=1}^{N_T}\int_{I_n}\|\dot{w}\|^2_{0,h}\,\mathrm{d}t = \sum_{n=1}^{N_T}\left\|M_h^{1/2}\mathbf{U}\right\|^2_{L^2(I_n)}$. We now focus on the terms in the second line of (6.1). We have

$$\begin{aligned}\|u^+_{h,\boldsymbol{\tau}}(0^+,\cdot)\|^2_{0,h} &= \|u_1\|^2_{0,h}(\dot{u}_2(0^+))^2 = \sum_{i,j=1}^{N_h}\left(U_i\dot{u}_2(0^+)\right)(M_h)_{i,j}\left(U_i\dot{u}_2(0^+)\right) \\ &= \left(M_h^{1/2}\dot{\mathbf{U}}(0^+)\right)^2,\end{aligned}$$

and, similarly, we find $\|u^+_{h,\boldsymbol{\tau}}(T^-,\cdot)\|^2_{0,h} = \left(M_h^{1/2}\dot{\mathbf{U}}(T^-)\right)^2$. Moreover,

$$\begin{aligned}\|[u^+_{h,\boldsymbol{\tau}}]_n\|^2_{0,h} &= \|u_1\|^2_{0,h}([\dot{u}_2]_n)^2 = \sum_{i,j=1}^{N_h}\left(U_i[\dot{u}_2]_n\right)(M_h)_{i,j}\left(U_i[\dot{u}_2]_n\right) \\ &= \left(M_h^{1/2}[\dot{\mathbf{U}}]_n\right)^2.\end{aligned}$$

We conclude observing that the terms in the third line of (6.1) can be treated analogously. □

Remark 6.2. Lemma 6.1 extends to $e_h := u_h - u_{h,\boldsymbol{\tau}}$, u_h being the solution to the semi-discrete problem (3.15).

Theorem 6.3 *(Error estimate). Let the assumptions of Theorem 3.6 and Theorem 4.1 hold. Then, there holds*

$$\begin{aligned}|||u-u_{h,\boldsymbol{\tau}}||| \lesssim\ & T\left[\sum_{n=1}^{N_T}\frac{\tau_n^{2\beta_n-3}}{r_n^{2q_n-6}}\left(|u_{h,0}|^2_{1,h} + \|z_{h,0}\|^2_{0,h} + |f_h|^2_{H^{q_n}(0,t;L^2(\Omega))}\right)\right]^{1/2} \\ & + T\,h^k\Bigg[|u_0|^2_{H^{k+1}(\Omega)} + h^2|z_0|^2_{H^{k+1}(\Omega)} + h^2|f|^2_{L^2(0,T;H^{k+1}(\Omega))} \\ & + |u_t|^2_{L^1(0,T;H^{k+1}(\Omega))} + h^2|u_t|^2_{L^2(0,T;H^{k+1}(\Omega))} \\ & + h^2|u_{tt}|^2_{L^1(0,T;H^{k+1}(\Omega))} + h^2|u_{tt}|^2_{L^2(0,T;H^{k+1}(\Omega))}\Bigg]^{1/2}.\end{aligned} \tag{6.2}$$

Proof. Let $u_h(t) \in C^0\left(0,T;W_h\right) \cap C^1\left(0,T;W_h\right)$ be the solution to the semi-discrete problem (3.15). Then, we split the error $e := u - u_{h,\boldsymbol{\tau}} = (u-u_h) + (u_h - u_{h,\boldsymbol{\tau}})$, where $e_h := u - u_h$ is the error due to the space

approximation by means of the VEM, and $e_\tau := u_h - u_{h,\tau}$ is the error due to the DG time discretization. By triangular inequality, we have

$$|||u - u_{h,\tau}||| \le |||e_h||| + |||e_\tau|||. \tag{6.3}$$

We start bounding the second contribution to the norm of the error. Applying Lemma 6.1 (and Remark 6.2) and Theorem 4.1, we find

$$|||e_\tau|||^2 \lesssim \sum_{n=1}^{N_T} \frac{\tau_n^{2\beta_n-3}}{r_n^{2q_n-6}} \|\mathbf{U}\|^2_{(H^{q_n}(I_n))^{N_h}},$$

and by definition of the $H^{q_n}(I_n)$-norm we get

$$|||e_\tau|||^2 \lesssim \sum_{n=1}^{N_T} \frac{\tau_n^{2\beta_n-3}}{r_n^{2q_n-6}} \int_{I_n} \left(\|u_h(t)\|^2_{L^2(\Omega)} + \cdots + \left\|\partial_t^{q_n} u_h(t)\right\|^2_{L^2(\Omega)} \right) \mathrm{d}t,$$

where $\partial_t^{q_n} u_h$ is the q_n-th time derivative of u_h. Applying the Poincaré inequality, (3.11) and Theorem 3.2, we find

$$\begin{aligned}\|u_h(t)\|^2_{L^2(\Omega)} &\lesssim |u_h(t)|^2_{H^1(\Omega)} \lesssim |u_h(t)|_{1,h} \\ &\lesssim \left(|u_{h,0}|^2_{1,h} + \|z_{h,0}\|^2_{0,h} + \|f_h\|^2_{L^2(0,t,L^2(\Omega))} \right),\end{aligned}$$

so that

$$\int_{I_n} \|u_h(t)\|^2_{L^2(\Omega)} \,\mathrm{d}t \lesssim T \left(|u_{h,0}|^2_{1,h} + \|z_{h,0}\|^2_{0,h} + \|f_h\|^2_{L^2(0,T,L^2(\Omega))} \right).$$

Similarly, applying the Poincaré inequality, (3.11) and Remark 3.3, for all $1 \le \alpha \le q_n$ integer, we obtain

$$\int_{I_n} \left\|\partial_t^{q_n} u_h(t)\right\|^2_{L^2(\Omega)} \,\mathrm{d}t \lesssim T \left\|\partial_t^{q_n} f_h\right\|^2_{L^2(0,T,L^2(\Omega))}.$$

Hence, we have shown that

$$|||e_\tau|||^2 \lesssim T \sum_{n=1}^{N_T} \frac{\tau_n^{2\beta_n-3}}{r_n^{2q_n-6}} \left(|u_{h,0}|^2_{1,h} + \|z_{h,0}\|^2_{0,h} + |f_h|^2_{H^{q_n}(0,T;L^2(\Omega))} \right). \tag{6.4}$$

We consider now the error due to the VEM approximation in space. Recalling that $e_h \in C^1(0,T;W_h)$, we have

$$\begin{aligned}|||e_h|||^2 = \sum_{n=1}^{N_T} \int_{I_n} \|\dot e_h\|^2_{0,h} \,\mathrm{d}t + \frac{1}{2}\|\dot e_h(0^+)\|^2_{0,h} + \frac{1}{2}\|\dot e_h(T^-)\|^2_{0,h} \\ + \frac{1}{2}|e_h(0^+)|^2_{1,h} + \frac{1}{2}|e_h(T^-)|^2_{1,h}.\end{aligned} \tag{6.5}$$

Since $u_{h,0}$ is the interpolant of degree k of u_0, thanks to (3.7) there holds

$$|e_h(0^+)|_{1,h} = |u_0 - u_{h,0}|_{1,h} \lesssim h^k |u_0|_{H^{k+1}(\Omega)}, \tag{6.6}$$

and similarly, since $z_{h,0}$ is the interpolant of degree k of z_0

$$\|\dot e_h(0^+)\|_{0,h} = \|z_0 - z_{h,0}\|_{0,h} \lesssim h^{k+1} |z_0|_{H^{k+1}(\Omega)}. \tag{6.7}$$

Using (3.11) and Theorem 3.6, we find:

$$\begin{aligned}&|e_h(T^-)|^2_{1,h} + \|\dot e_h(T^-)\|^2_{0,h} = |u(T^-) - u_h(T^-)|^2_{1,h} + \|u_t(T^-) - u_{h,t}(T^-)\|^2_{0,h} \\ &\lesssim \|u(T^-) - u_h(T^-)\|^2_{H^1(\Omega)} + \|u_t(T^-) - u_{h,t}(T^-)\|^2_{L^2(\Omega)} \\ &\lesssim h^{2k}\Big(|u_0|^2_{H^{k+1}(\Omega)} + h^2 |z_0|^2_{H^{k+1}(\Omega)} + h^2 |f|^2_{L^2(0,T;H^{k+1}(\Omega))} \\ &\quad + |u_t|^2_{L^1(0,T;H^{k+1}(\Omega))} + h^2 |u_t|^2_{L^2(0,T;H^{k+1}(\Omega))} + h^2 |u_{tt}|^2_{L^1(0,T;H^{k+1}(\Omega))} \\ &\quad + h^2 |u_{tt}|^2_{L^2(0,T;H^{k+1}(\Omega))} \Big).\end{aligned} \tag{6.8}$$

Finally, thanks to (3.11) and Theorem 3.6, we find:

$$\begin{aligned}&\int_{I_n} \|\dot e_h(s)\|^2_{0,h} \,\mathrm{d}s = \int_{I_n} \|u_t(s) - u_{h,t}(s)\|^2_{0,h} \,\mathrm{d}s \lesssim \int_{I_n} \|u_t(s) - u_{h,t}(s)\|^2_{L^2(\Omega)} \,\mathrm{d}s \\ &\lesssim \tau_n h^{2k}\Big(|u_0|^2_{H^{k+1}(\Omega)} + h^2 |z_0|^2_{H^{k+1}(\Omega)} + h^2 |f|^2_{L^2(0,T;H^{k+1}(\Omega))} \\ &\quad + |u_t|^2_{L^1(0,T;H^{k+1}(\Omega))} + h^2 |u_t|^2_{L^2(0,T;H^{k+1}(\Omega))} + h^2 |u_{tt}|^2_{L^1(0,T;H^{k+1}(\Omega))} \\ &\quad + h^2 |u_{tt}|^2_{L^2(0,T;H^{k+1}(\Omega))} \Big).\end{aligned} \tag{6.9}$$

Inserting (6.6), (6.7), (6.8) and (6.9) into (6.5), and using that $\sum_{n=1}^{N_T} \tau_n = T$, we obtain

$$\begin{aligned}|||e_h|||^2 \lesssim T h^{2k}\Big(&|u_0|^2_{H^{k+1}(\Omega)} + h^2 |z_0|^2_{H^{k+1}(\Omega)} + h^2 |f|^2_{L^2(0,T;H^{k+1}(\Omega))} \\ &+ |u_t|^2_{L^1(0,T;H^{k+1}(\Omega))} + h^2 |u_t|^2_{L^2(0,T;H^{k+1}(\Omega))} + h^2 |u_{tt}|^2_{L^1(0,T;H^{k+1}(\Omega))} \\ &+ h^2 |u_{tt}|^2_{L^2(0,T;H^{k+1}(\Omega))} \Big).\end{aligned} \tag{6.10}$$

The final result (6.2) follows from (6.4) and (6.10). □

Corollary 6.4. *Let $u \in C^2\left(0,T;H^1_0(\Omega) \cap H^{k+1}(\Omega)\right)$, $u_0, z_0 \in H^{k+1}(\Omega)$ and $u_t, u_{tt}, f \in L^2\left(0,T;H^{k+1}(\Omega)\right)$, with $k \ge 1$ integer. Moreover, let $u \in H^q\left(I_n;H^1_0(\Omega)\right)$ for all $n = 1,\dots,N_T$, with $q \ge 2$, with $\tau_n = \Delta t > 0$ and $r_n = r \in \mathbb{N}$ for all $n = 1,\dots,N_T$. Then,*

$$|||u - u_{h,\tau}||| = O(\Delta t^{\beta - 3/2} + h^k)$$

as Δt and h decrease to 0.

7. Numerical tests

All the numerical tests are performed in Matlab, and make use of the VEM code available at [50] for spatial discretization. For DG in time, we refer to [21]. The meshes are generated using the code Polymesher [51].

7.1. Verification test

As verification test, we consider equation (2.1) on $\Omega \times (0,T] = (0,1)^2 \times (0,1]$, where $\nu = 1$ and the loading term f as well as the initial conditions u_0, z_0 are chosen so that

$$u_{ex}(t,x_1,x_2) := \sin(t^2)\sin(\pi x_1)\sin(\pi x_2) \tag{7.1}$$

is the unique solution of the problem (see Fig. 7.1).

First, we verify the convergence of the VEM-DG error as the time discretization refines. We compute the VEM-DG solution $u_{h,\tau}$ applying the VEM of degree $k = 4$ on the Voronoi mesh represented in Fig. 7.2(a), coupled with the DG method in time over uniform partitions of $[0,1]$ with decreasing length Δt of the time-slabs and with varying polynomial degree $r = 1, 2, 3$. Note that the case $r = 1$ is not covered by the theory of Section 4. In Fig. 7.2(b) we observe the expected decay of the error at final time, namely, $|||u_{ex}(T) - u_{h,\tau}(T)||| = O(\Delta t^{r-1/2})$ (see Corollary 4.2).

In the second experiment, we study the convergence of the VEM-DG error as the space discretization refines. To this end, we consider the DG approximation of degree $r = 6$ over the uniform partition of $[0,1]$ with $\Delta t = 0.1$, coupled with the VEM on different Voronoi meshes (see Fig. 7.3) and with increasing degree $k = 1, 2, 3$. In Fig. 7.4(a) the expected behavior $|||u_{ex}(T) - u_{h,\tau}(T)||| = O(h^k)$ is observed (see Theorem 3.6).

Finally, in the last experiment, we take $r = k$ and $h \sim \Delta t$. The error decay is depicted in Fig. 7.4(b), and it is in agreement with (6.2).

7.2. Validation test

The second experiment deals with a more realistic scenario, and aims at investigating the performances of the proposed numerical

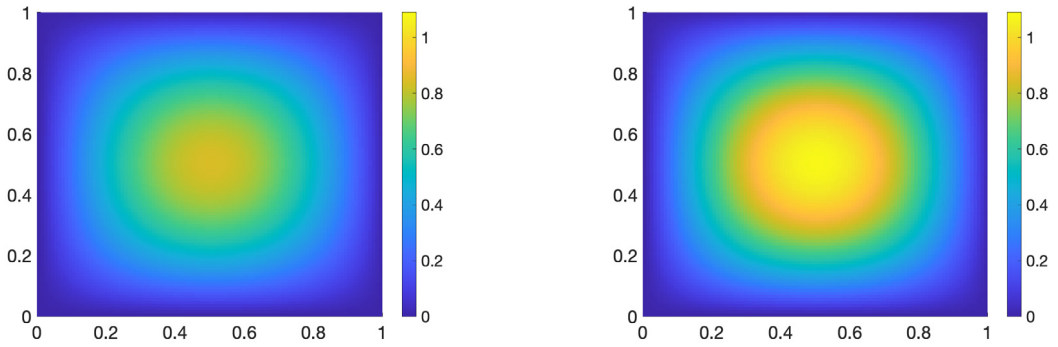

Fig. 7.1. (a) u_{ex} at final time $T = 1$; (b) $u_{ex,t}$ at final time $T = 1$.

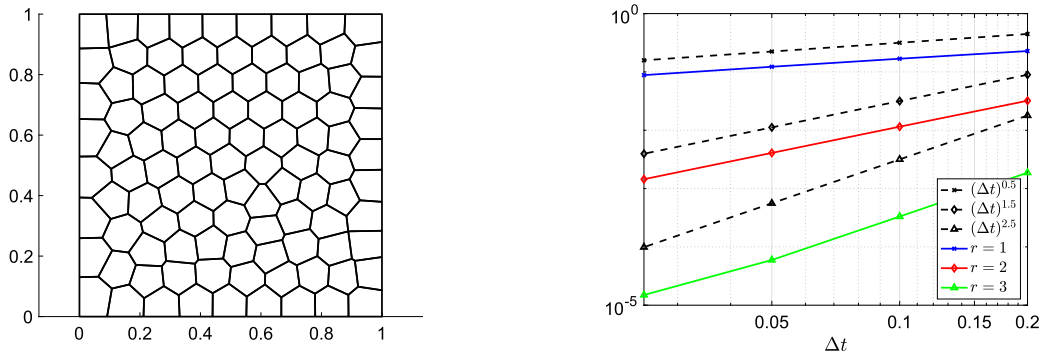

Fig. 7.2. (a) Voronoi mesh with 100 polygonal elements; (b) $|||u_{ex}(T) - u_{h,\tau}(T)|||$, where $u_{h,\tau}$ is computed using VEM of degree $k = 4$ and DG of increasing degree $r = 1, 2, 3$.

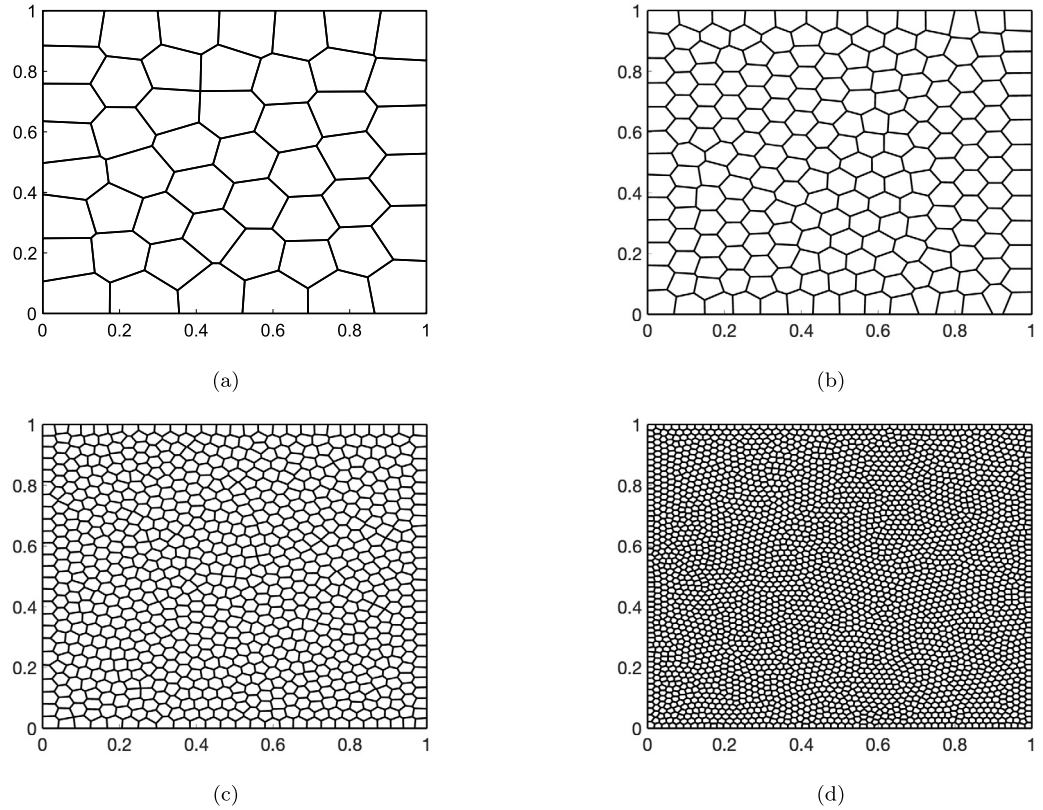

Fig. 7.3. Voronoi meshes with 50 (top left) 200 (top right) 800 (bottom left) and 3200 (bottom right) elements.

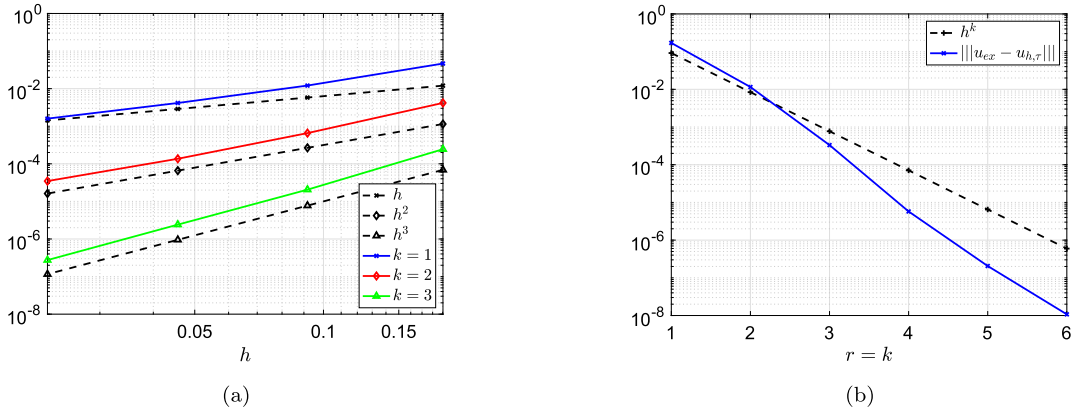

Fig. 7.4. (a) $|||u_{ex}(T)-u_{h,\tau}(T)|||$, where $u_{h,\tau}$ is computed using DG of degree $r=6$ on a uniform partition of the time interval with $\Delta t=0.01$ and VEM of increasing degree $k=1,2,3$. (b) $|||u_{ex}(T)-u_{h,\tau}(T)|||$, where $u_{h,\tau}$ is computed using DG on a uniform partition of the time interval with $\Delta t=0.1$ and VEM on the Voronoi mesh with 200 elements (see Fig. 7.3(b), with equal degree in time and space).

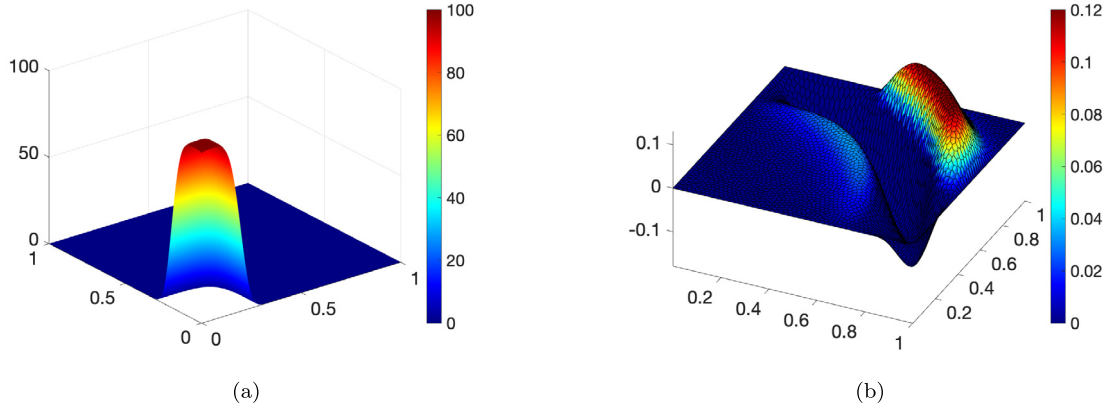

Fig. 7.5. (a) Loading term (7.2). (b) Reference solution.

scheme in the non-dissipative case, which is not covered by the theory here developed. In particular, we consider problem (2.1) with $\nu=0$, initial data $u_0\equiv 0$, $z_0\equiv 0$ and loading term

$$f(t,x)=\begin{cases}100\,e^{-\frac{(x-x_0)^4}{s^2}} & \text{for } t<0.1\\ 0 & \text{else}\end{cases} \tag{7.2}$$

representing a smooth impulse centered at $x_0=(0.05,0.05)$, with $s=0.025$ (see Fig. 7.5(a)). For such example, there is no analytical solution. Hence, we refer to an overkilled solution computed by means of the VEM of degree 2 on a spatial mesh with 3200 elements coupled with DG for time discretization, with polynomial degree 2 and $\Delta t=1/320$ (see Fig. 7.5(b)).

In Fig. 7.6 we represent the snapshots at final time $T=1$ of the approximated solution obtained by means of the proposed VEM-DG strategy (the parameters for time integration are $\Delta t=1/20$ and $r=2$), compared with the approximations produced using the Newmark method for increasing Δt. Note that the numerical scheme for the space integration is the same as in the reference solution. We can observe that the discrete solution computed with Newmark is affected by spurious oscillations. In Fig. 7.7 we report the computed time history of the displacement on a receiver located at $(0.5,0.5)$. It is clear that the VEM-DG approximation is more accurate than those computed with the Newmark method. Finally, in Fig. 7.8 we represent the history of the displacement on a receiver located at $(0.5,0.5)$ (left) and $(0.2,0.2)$ (right), for varying multiplicative coefficient (chosen equal to 0.1, 1 and 10) in front of the stability bilinear forms $S_h(\bullet,\bullet)$ and $R_h(\bullet,\bullet)$. The time integration is performed by means of Newmark's method with $\Delta t=1/80$. In both figures, no substantial difference between the three lines obtained by means of Newmark's method can be appreciated.

Data availability

No data was used for the research described in the article.

Acknowledgements

PFA, FB and MV are members of the INdAM Research group GNCS. FB is partially funded by "INdAM – GNCS Project", codice CUP_E53C22001930001. PFA and MV are partially funded by the Italian Ministry of Universities and Research (MUR), research grant PRIN2020 n. 20204LN5N5. FA and MV are partially funded by the Italian Ministry of Universities and Research (MUR), research grant PRIN2017 n. 201744KLJL. PFA is partially supported by ICSC – Centro Nazionale di Ricerca in High Performance Computing, Big Data, and Quantum Computing funded by European Union – NextGenerationEU. The present research is part of the activities of "Dipartimento di Eccellenza 2023-2027".

Appendix A. Representation formula for the semi-discrete solution

Theorem Appendix A.1. *The unique solution to problem (3.15) is given by*

$$u_h(t):=\sum_{n=1}^{N_h}\gamma_n(t)w_h^{(n)}, \tag{A.1}$$

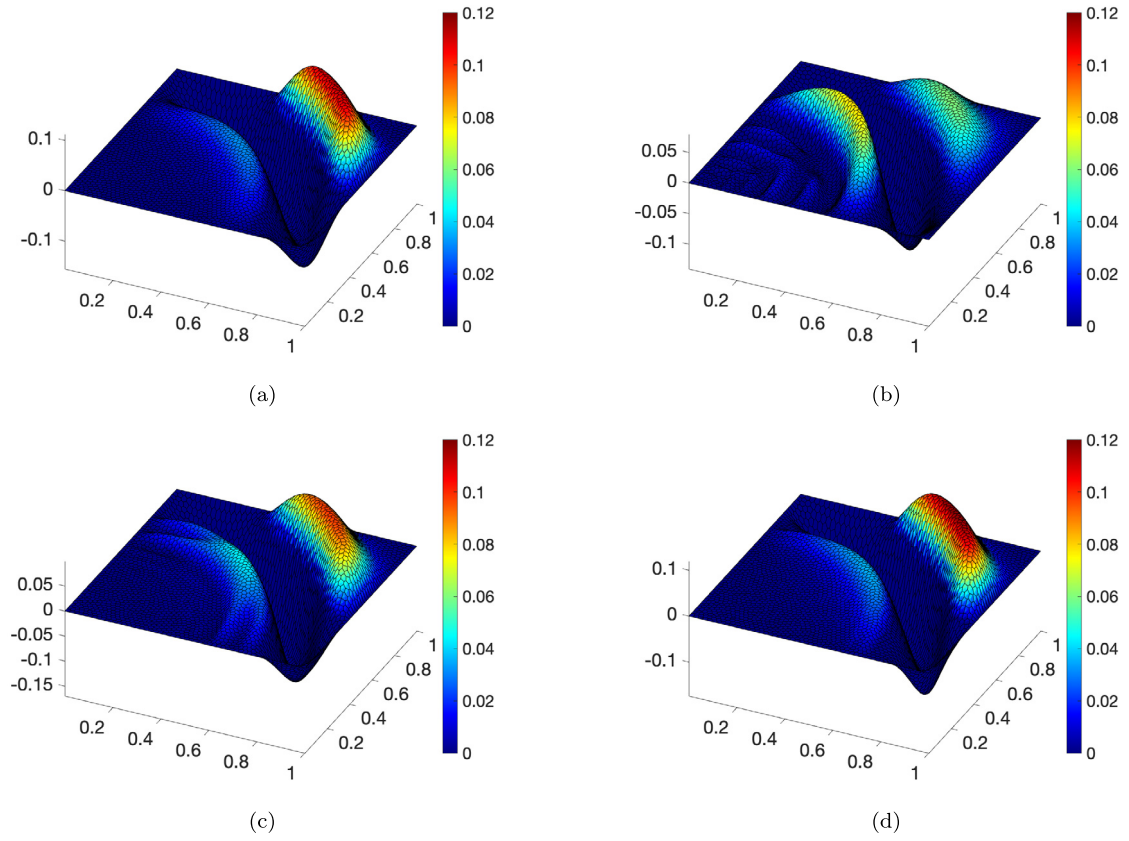

Fig. 7.6. Fully discrete solution computed by means of the proposed VEM-DG strategy with $\Delta t = 1/20$ and $r = 2$ (a) compared with the numerical approximation obtained by means of VEM in space coupled with Newmark for time integration, with $\Delta t = 1/20$ (b), $\Delta t = 1/40$ (c) and $\Delta t = 1/80$ (d).

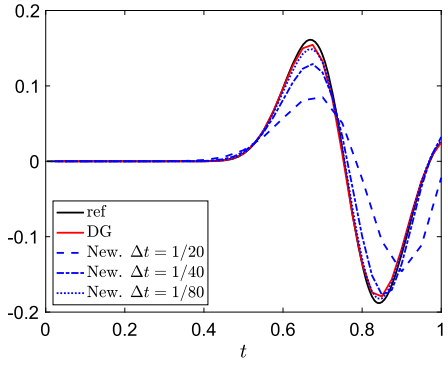

Fig. 7.7. Computed time history of the displacement on a receiver located at $(0.5, 0.5)$. The black line represents the reference solution. The red line represents the VEM-DG solution. The dashed blue lines represent the solutions computed with the Newmark method for increasing Δt.

where $\{w_h^{(n)}\}_{n=1}^{N_h}$ *is the basis of* W_h *orthonormal with respect to* $m_h(\bullet,\bullet)$ *fulfilling, for all* $v_h \in W_h$ *and for all* $n = 1, \dots, N_h$

$$a_h(w_h^{(n)}, v_h) = \lambda_h^{(n)} m_h(w_h^{(n)}, v_h),$$

with $0 < \lambda_h^{(1)} \le \cdots \le \lambda_h^{(N_h)}$*, and the n-th coefficient in the eigen-expansion of* $u_h(t)$ (A.1) *is given by*

$$\gamma_n(t) := e^{-\nu/2t}\left[m_h(u_{h,0}, w_h^{(n)})\cos(\omega_h^{(n)} t) + \frac{1}{\omega_h^{(n)}} m_h(z_{h,0}, w_h^{(n)})\sin(\omega_h^{(n)} t) + \frac{1}{\omega_h^{(n)}} \int_0^t e^{-\nu/2(t-s)} \sin(\omega_h^{(n)}(t-s)) \left(f_h(s), w_h\right)_{L^2(\Omega)} ds \right] \tag{A.2}$$

where $\omega_h^{(n)} := \sqrt{\lambda_h^{(n)} - \frac{\nu^2}{4}}$*, with* ν *being small enough so that* $\lambda_h^{(n)} - \frac{\nu^2}{4} > 0$ *for all* $n = 1, \dots, N_h$.

To prove Theorem Appendix A.1 we need two auxiliary results.

Lemma Appendix A.2. *Let*

$$F_n(t) := e^{-\nu/2t}\left(c_n \cos(\omega_h^{(n)} t) + \frac{d_n}{\omega_h^{(n)}} \sin(\omega_h^{(n)} t)\right), \tag{A.3}$$

with c_n, $d_n > 0$*. Then, there holds*

$$\ddot{F}_n(t) + \nu \dot{F}_n(t) + \lambda_h^{(n)} F_n(t) = 0, \tag{A.4}$$

where $\lambda_h^{(n)}, \omega_h^{(n)}$ *have been defined in Theorem 3.2.*

Proof. Equation (A.4) follows by observing that

$$\dot{F}(t) = e^{-\nu/2t}\left[\left(-\frac{\nu}{2} c_n + d_n \right)\cos(\omega_h^{(n)} t) + \left(-\frac{\nu}{2}\frac{c_n}{\omega_h^{(n)}} - c_n \omega_h^{(n)} \right)\sin(\omega_h^{(n)} t) \right],$$

$$\ddot{F}(t) = e^{-\nu/2t}\left[\left(\frac{\nu^2}{4} c_n - \nu d_n - c_n (\omega_h^{(n)})^2 \right)\cos(\omega_h^{(n)} t) + \left(\frac{\nu^2}{4}\frac{d_n}{\omega_h^{(n)}} + \nu c_n \omega_h^{(n)} - \omega_h^{(n)} d_n \right)\sin(\omega_h^{(n)} t) \right]. \quad \square$$

Lemma Appendix A.3. *Let*

$$G_n(t) := \int_0^t g_n(t,s)\, ds, \tag{A.5}$$

with

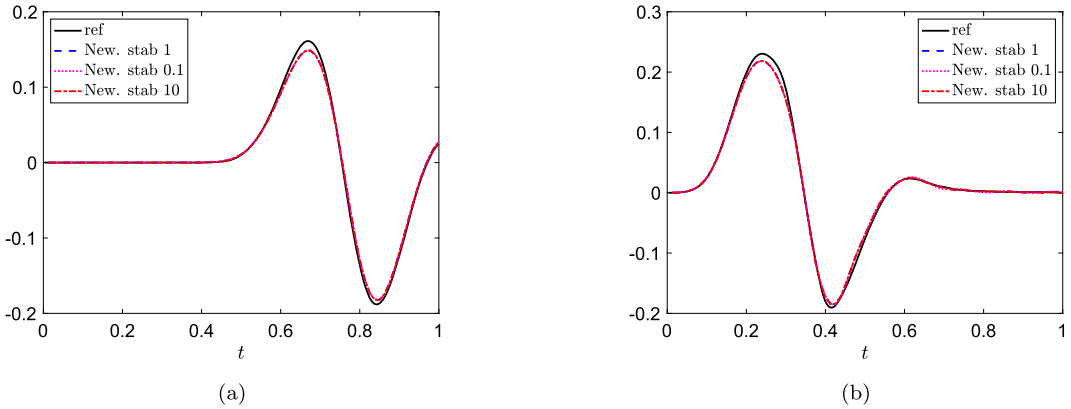

Fig. 7.8. Computed time history of the displacement on a receiver located at $(0.5, 0.5)$ (a) and at $(0.2, 0.2)$ (b) for varying stability coefficient. The time integration is performed by means of Newmark's method with $\Delta t = 1/80$.

$$g_n(t,s) := \frac{1}{\omega_h^{(n)}} e^{-\nu/2(t-s)} \sin(\omega_h^{(n)}(t-s)) \left(f_h(s), w_h\right)_{L^2(\Omega)}. \tag{A.6}$$

Then, there holds

$$\ddot{G}_n(t) + \nu \dot{G}_n(t) + \lambda_h^{(n)} G_n(t) = \left(f_h(t), w_h\right)_{L^2(\Omega)}, \tag{A.7}$$

where $\lambda_h^{(n)}, \omega_h^{(n)}$ have been defined in Theorem 3.2.

Proof. We note that

$$\frac{d}{dt}\int_0^t g(s,t)\,ds = g(t,t) - g(0,t) + \int_0^t \frac{\partial}{\partial t} g(s,t)\,ds,$$

$$\frac{d^2}{dt^2}\int_0^t g(s,t)\,ds = \frac{d}{dt}\Big(g(t,t) - g(0,t)\Big) + \frac{\partial}{\partial t} g(s,t)|_{s=t} - \frac{\partial}{\partial t} g(s,0) + \int_0^t \frac{\partial^2}{\partial t^2} g(s,t)\,ds.$$

Equation (A.7) follows by choosing $f(0) = 0$ and observing that

$$\dot{G}(t) = \int_0^t e^{-\nu/2(t-s)} \left[-\frac{\nu}{2\omega_h^{(n)}} \sin(\omega_h^{(n)}(t-s)) + \cos(\omega_h^{(n)}(t-s)) \right] \times \left(f_h(s), w_h\right)_{L^2(\Omega)} ds,$$

and

$$\ddot{G}(t) = \left(f_h(t), w_h\right)_{L^2(\Omega)} + \int_0^t e^{-\nu/2(t-s)} \left(f_h(s), w_h\right)_{L^2(\Omega)} \left[-\nu \cos(\omega_h^{(n)}(t-s)) + \left(\frac{\nu^2}{4\omega_h^{(n)}} - \omega_h^{(n)} \right) \sin(\omega_h^{(n)}(t-s)) \right] ds. \quad \square$$

Proof of Theorem Appendix A.1. Since $\{w_h^{(n)}\}_{n=1}^{N_h}$ is the basis of W_h, it is enough to verify that (A.1) fulfills problem (3.15) for all test functions $v_h = w_h^{(n)}$, with $n = 1, \dots, N_h$. Observe that

$$a_h(u_h(t), w_h^{(n)}) = \sum_{m=1}^{N_h} \gamma_n(t) a_h(w_h^{(m)}, w_h^{(n)}) = \begin{cases} 0, & \text{if } n \neq m, \\ \gamma_n(t)\lambda_h^{(n)} \left\| w_h^{(n)} \right\|_{0,h}^2 = \lambda_h^{(n)} \gamma_n(t), & \text{if } n = m, \end{cases}$$

and, analogously, $m_h(u_h(t), w_h^{(n)}) = \gamma_n(t)$. Then,

$$m_h(u_{h,tt}(t), w_h^{(n)}) + \nu m_h(u_{h,t}(t), w_h^{(n)}) + a_h(u_h(t), w_h^{(n)}) = \frac{d^2}{dt^2} m_h(u_h(t), w_h^{(n)}) + \nu \frac{d}{dt} m_h(u_h(t), w_h^{(n)}) + a_h(u_h(t), w_h^{(n)}) = \frac{d^2}{dt^2}\gamma_n(t) + \nu \frac{d}{dt}\gamma_n(t) + \lambda_h^{(n)}\gamma_n(t). \tag{A.8}$$

We conclude that (A.8) $= \left(f_h(t), w_h\right)_{L^2(\Omega)}$ by applying Lemma Appendix A.2, since $\gamma_n(t) = F_n(t) + G_n(t)$, where $F_n(t)$ is of the form (A.3) - the constants being fixed so that $u_h(t)$ fulfills the initial conditions $u_h(0) = u_{h,0}$, $u_{h,t}(0) = z_{h,0}$, namely,

$$c_n = m_h(u_{h,0}, w_h^{(n)}), \quad d_n = \frac{1}{\omega_h^{(n)}} m_h(z_{h,0}, w_h^{(n)}),$$

and by applying Lemma Appendix A.3, since $G_n(t)$ is of the form (A.5)-(A.6). $\square$

References

[1] L. Beirão da Veiga, F. Brezzi, A. Cangiani, G. Manzini, L.D. Marini, A. Russo, Basic principles of Virtual Element Methods, Math. Models Methods Appl. Sci. 23 (01) (2013) 199–214.

[2] L. Beirão da Veiga, F. Brezzi, L.D. Marini, Virtual Elements for linear elasticity problems, SIAM J. Numer. Anal. 51 (2) (2013) 794–812.

[3] A.L. Gain, C. Talischi, G.H. Paulino, On the Virtual Element Method for three-dimensional linear elasticity problems on arbitrary polyhedral meshes, Comput. Methods Appl. Mech. Eng. 282 (2014) 132–160.

[4] L. Beirão da Veiga, C. Lovadina, D. Mora, A Virtual Element Method for elastic and inelastic problems on polytope meshes, Comput. Methods Appl. Mech. Eng. 295 (2015) 327–346.

[5] G. Vacca, L. Beirão da Veiga, Virtual element methods for parabolic problems on polygonal meshes, Numer. Methods Partial Differ. Equ. 31 (6) (2015) 2110–2134.

[6] F. Brezzi, L.D. Marini, Virtual Element Methods for plate bending problems, Comput. Methods Appl. Mech. Eng. 253 (2013) 455–462.

[7] P.F. Antonietti, L. Beirão da Veiga, S. Scacchi, M. Verani, A C^1 Virtual Element Method for the Cahn-Hilliard equation with polygonal meshes, SIAM J. Numer. Anal. 54 (1) (2016) 34–56.

[8] P.F. Antonietti, L. Beirão da Veiga, D. Mora, M. Verani, A stream Virtual Element formulation of the Stokes problem on polygonal meshes, SIAM J. Numer. Anal. 52 (1) (2014) 386–404.

[9] I. Perugia, P. Pietra, A. Russo, A plane wave Virtual Element Method for the Helmholtz problem, ESAIM: Math. Model. Numer. Anal. 50 (3) (2016) 783–808.

[10] M. Frittelli, I. Sgura, Virtual Element Method for the Laplace Beltrami equation on surfaces, ESAIM: Math. Model. Numer. Anal. 52 (3) (2018) 965–993.

[11] G. Vacca, Virtual element methods for hyperbolic problems on polygonal meshes, Comput. Math. Appl. 74 (5) (2017) 882–898.

[12] P.F. Antonietti, G. Manzini, I. Mazzieri, H.M. Mourad, M. Verani, The arbitrary-order virtual element method for linear elastodynamics models: convergence, stability and dispersion-dissipation analysis, Int. J. Numer. Methods Eng. 122 (4) (2021) 934–971.

[13] P.F. Antonietti, G. Manzini, I. Mazzieri, S. Scacchi, M. Verani, The conforming virtual element method for polyharmonic and elastodynamics problems: a review, in: The Virtual Element Method and Its Applications, in: SEMA SIMAI Springer Ser., vol. 31, Springer, Cham, 2022, pp. 411–451, ©2022.

[14] F. Dassi, A. Fumagalli, I. Mazzieri, A. Scotti, G. Vacca, A virtual element method for the wave equation on curved edges in two dimensions, J. Sci. Comput. 90 (50) (2022).

[15] R.J. Le Veque, Finite Difference Methods for Ordinary and Partial Differential Equations, SIAM - Society for Industrial and Applied Mathematics, 2007.
[16] J.C. Butcher, Numerical Methods for Ordinary Differential Equations, Wiley, 2008.
[17] T. Tezduyar, S. Sathe, R. Keedy, K. Stein, Space–time finite element techniques for computation of fluid–structure interactions, Comput. Methods Appl. Mech. Eng. 195 (2006) 2002–2027.
[18] O. Steinbach, M. Zank, A stabilized space–time finite element method for the wave equation, in: Advanced Finite Element Methods with Applications, 2017, pp. 341–370.
[19] J. Ernesti, C. Wieners, Space-time discontinuous Petrov–Galerkin methods for linear wave equations in heterogeneous media, Comput. Methods Appl. Math. 19 (2019) 465–481.
[20] P. Bansal, A. Moiola, I. Perugia, C. Schwab, Space–time discontinuous Galerkin approximation of acoustic waves with point singularities, IMA J. Numer. Anal. 41 (3) (2020) 2056–2109.
[21] P.F. Antonietti, I. Mazzieri, F. Migliorini, A space-time discontinuous Galerkin method for the elastic wave equation, J. Comput. Phys. 419 (2020) 109685.
[22] E.H. Georgoulis, O. Lakkis, T.P. Wihler, A posteriori error bounds for fully-discrete hp-discontinuous Galerkin timestepping methods for parabolic problems, Numer. Math. 148 (2021) 363–386.
[23] A. Cangiani, E. Georgoulis, S. Giani, S. Metcalfe, hp-adaptive discontinuous Galerkin methods for non-stationary convection–diffusion problems, Comput. Math. Appl. 78 (9) (2019) 3090–3104, applications of Partial Differential Equations in Science and Engineering.
[24] T. Hughes, G. Hulbert, Space-time finite element methods for elastodynamics: formulation and error estimates, Comput. Methods Appl. Mech. Eng. 66 (1988) 339–363.
[25] A. Idesman, Solution of linear elastodynamics problems with space–time finite elements on structured and unstructured meshes, Comput. Methods Appl. Mech. Eng. 196 (2007) 1787–1815.
[26] L. Yin, A. Acharya, N. Sobh, R.B. Haber, D.A. Tortorelli, A space-time discontinuous Galerkin method for elastodynamic analysis, in: B. Cockburn, G.E. Karniadakis, C.-W. Shu (Eds.), Discontinuous Galerkin Methods, Springer Berlin Heidelberg, 2000, pp. 459–464.
[27] R. Abedi, B. Petracovici, R.B. Haber, A space–time discontinuous Galerkin method for linearized elastodynamics with element-wise momentum balance, Comput. Methods Appl. Mech. Eng. 195 (2006) 3247–3273.
[28] W. Dörfler, S. Findeisen, C. Wieners, Space-time discontinuous Galerkin discretizations for linear first-order hyperbolic evolution systems, Comput. Methods Appl. Math. 16 (2016) 409–428.
[29] S. Gómez, L. Mascotto, A. Moiola, I. Perugia, Space-time virtual elements for the heat equation, arXiv preprint, arXiv:2212.05343, 2022.
[30] F. Kretzschmar, A. Moiola, I. Perugia, S.M. Schenpp, A priori error analysis of space-time Trefftz discontinuous Galerkin methods for wave problems, IMA J. Numer. Anal. 36 (2016) 1599–1635.
[31] L. Banjai, E.H. Georgoulis, O. Lijoka, A Trefftz polynomial space-time discontinuous Galerkin method for the second order wave equation, SIAM J. Numer. Anal. 55 (2017) 63–86.
[32] H. Barucq, H. Calandra, J. Diaz, E. Shishenina, Space–time Trefftz-DG approximation for elasto-acoustics, Appl. Anal. 99 (2018) 747–760.
[33] A. Moiola, I. Perugia, A space-time Trefftz discontinuous Galerkin method for the acoustic wave equation in first-order formulation, Numer. Math. 138 (2) (2018) 389–435.
[34] I. Perugia, J. Schöberl, P. Stocker, C. Wintersteiger, Tent pitching and Trefftz-DG method for the acoustic wave equation, Comput. Math. Appl. 79 (10) (2020) 2987–3000.
[35] J. Gopalakrishnan, J. Schöberl, C. Wintersteiger, Mapped tent pitching schemes for hyperbolic systems, Comput. Methods Sci. Eng. 39 (2017) B1043–B1063.
[36] J. Gopalakrishnan, P. Monk, P. Sepúlveda, A tent pitching scheme motivated by Friedrichs theory, Comput. Math. Appl. 70 (5) (2015) 1114–1135.
[37] C. Johnson, Discontinuous Galerkin finite element methods for second order hyperbolic problems, Comput. Methods Appl. Mech. Eng. 107 (1) (1993) 117–129.
[38] S. Adjerid, H. Temimi, A discontinuous Galerkin method for the wave equation, Comput. Methods Appl. Mech. Eng. 200 (5) (2011) 837–849.
[39] M. Delfour, W. Hager, F. Trochu, Discontinuous Galerkin methods for ordinary differential equations, Math. Comput. 36 (154) (1981) 455–473.
[40] J. van der Vegt, C. Klaji, F. van der Bos, H. van der Ven, Space-time discontinuous Galerkin method for the compressible Navier-Stokes equations on deforming meshes, in: European Conference on Computational Fluid Dynamics ECCOMAS CFD 2006, 2006.
[41] T. Werder, K. Gerder, D. Schötzau, C. Schwab, hp-discontinuous Galerkin time stepping for parabolic problems, Comput. Methods Appl. Mech. Eng. 190 (2001) 6685–6708.
[42] D.A. French, A space-time finite element method for the wave equation, Comput. Methods Appl. Mech. Eng. 107 (1) (1993) 145–157.
[43] D. He, L.L. Thompson, Adaptive space–time finite element methods for the wave equation on unbounded domains, Comput. Methods Appl. Mech. Eng. 194 (2005) 1947–2000.
[44] P.F. Antonietti, I. Mazzieri, F. Migliorini, A discontinuous Galerkin time integration scheme for second order differential equations with applications to seismic wave propagation problems, Comput. Math. Appl. 134 (2023) 87–100.
[45] G. Duvaut, J.L. Lions, Inequalities in Mechanics and Physics, vol. 219, Springer Science & Business Media, 2012.
[46] B. Ahmad, A. Alsaedi, F. Brezzi, L. Marini, A. Russo, Equivalent projectors for virtual element methods, Comput. Math. Appl. 66 (3) (2013) 376–391.
[47] L. Beirão da Veiga, F. Brezzi, L.D. Marini, A. Russo, The Hitchhiker's guide to the virtual element method, Math. Models Methods Appl. Sci. 24 (08) (2014) 1541–1573.
[48] S.C. Brenner, L.R. Scott, The Mathematical Theory of Finite Element Methods, vol. 3, Springer, 2008.
[49] P.F. Antonietti, I. Mazzieri, N. Dal Santo, A. Quarteroni, A high-order discontinuous Galerkin approximation to ordinary differential equations with applications to elastodynamics, IMA J. Numer. Anal. 38 (4) (2017) 1709–1734.
[50] vem-implementation-example, https://github.com/andrea-borio/vem-implementation-example, 2020.
[51] C. Talischi, G.H. Paulino, A. Pereira, I.F.M. Menezes, PolyMesher: a general-purpose mesh generator for polygonal elements written in Matlab, Struct. Multidiscip. Optim. 45 (3) (2012) 309–328.
[52] D. Mora, G. Rivera, R. Rodríguez, A virtual element method for the Steklov eigenvalue problem, Math. Models Methods Appl. Sci. 25 (08) (2015) 1421–1445.
[53] L. Chen, J. Huang, Some error analysis on virtual element methods, Calcolo 55 (1) (2018).
[54] L. Beirão da Veiga, C. Lovadina, A. Russo, Stability analysis for the virtual element method, Math. Models Methods Appl. Sci. 27 (13) (2017) 2557–2594.
[55] S.C. Brenner, L.-Y. Sung, Virtual element methods on meshes with small edges or faces, Math. Models Methods Appl. Sci. 28 (07) (2018) 1291–1336.
[56] C. Canuto, M.Y. Hussaini, A. Quarteroni, T.A. Zang, Spectral Methods: Evolution to Complex Geometries and Applications to Fluid Dynamics, Springer Science & Business Media, 2007, Sec. 2.3.